N-Acetylcysteine:
A new drug for Thrombotic
Thrombocytopenic Purpura?

Charlotte DEKIMPE

Promotor: Prof. dr. K. Vanhoorelbeke

Mentor: *Dr. C. Tersteeg*

Thesis presented in
fulfillment of the requirements
for the degree of Master of Science
in Biochemie & Biotechnologie

Academic year 2015-2016

Acknowledgement

Over the past year, I have worked on the effect of N-acetylcysteine on TTP symptoms. Finishing this research project would not have been possible without the support of many people. Therefore, I would like to say some words of thanks.

First of all, I would like to thank my promotor Prof. Dr. Karen Vanhoorelbeke for giving me the opportunity to make my dissertation in the Laboratory for Thrombosis Research group.

I am especially grateful to my mentor Claudia. Despite her busy schedule, she learned me a lot of new techniques, performed the animal experiments and corrected my dissertation very carefully.

I must also acknowledge all the PhD students of the Laboratory for Thrombosis Research, for being prepared to help when needed and for making the working environment more agreeable. I also want to thank the lab technicians, Inge, Aline, Nele and Linda, for answering all my questions and learning me several techniques and Katleen for taking care of the mice. Furthermore, I want to thank my fellow student Chloë, for the nice break moments.

I also want to thank my parents, brother and sister for supporting me during these five years of studies. Last, but certainly not least, Joren, thanks for your endless patience and support during all these years.

Summary

Thrombotic thrombocytopenic purpura (TTP) is a rare and life-threatening microangiopathic disease, caused by a deficiency in the Von Willebrand factor (VWF)-cleaving metalloprotease ADAMTS13. Current treatment strategies for TTP exist of plasma infusion for congenital TTP and plasma exchange, often combined with immunosuppressive therapies, for acquired TTP. Although plasma therapy has strongly increased the patient's survival rate, this treatment also has major disadvantages. Therefore, new therapies for TTP are still desirable. The anti-mucolytic drug N-acetylcysteine (NAC) could be a possible new treatment strategy for acute TTP, as it has been proven to reduce VWF multimer size.

In this thesis, the viability of NAC for the prevention and treatment of acute TTP symptoms was investigated by means of a mouse model for congenital TTP.

TTP was triggered in $Adamts13^{-/-}$ mice by injection of 2000-2250 U/kg recombinant VWF (rVWF). In this model, 800 mg/kg NAC was administered prophylactic (15 min before rVWF injection) or as a treatment (1 and 12 hours after rVWF injection) for TTP. Blood- and plasma samples were analysed for the presence of TTP symptoms, including thrombocytopenia, hemolytic anemia and tissue damage.

The prophylactic administration of NAC did prevent the onset of TTP symptoms in mice. Twenty-four hours after rVWF injection, platelet counts and hemoglobin levels were significantly higher in mice that received NAC compared to control mice, whereas LDH activity levels where signifcantly lower. However, the administration of NAC could not resolve already existing TTP symptoms effectively. Nevertheless, NAC could reduce VWF size in circulation of both mice groups that received NAC, but it could not break down VWF in already existing platelet agglutinates in vitro.

NAC was found to be effective in preventing TTP, but not in curing already existing TTP symptoms in mice.

Samenvatting

Thrombotische trombocytopenische purpura (TTP) is een zeldame en levensbedreigende microangiopathische ziekte die wordt veroorzaakt door een deficiëntie van het von Willebrand factor (VWF)-knippend metalloprotease ADAMTS13. Huidige behandelingen voor TTP bestaan uit plasma infusie voor congenitale TTP en plasma uitwisseling, vaak in combinatie met immunosuppressietherapieën, voor verworven TTP. Alhoewel plasmatherapie de overlevingskans sterk heeft doen stijgen, zijn er ook ernstige nadelen aan deze behandeling. Daarom moet er nog steeds op zoek worden gegaan naar nieuwe behandelingen. Het anti-mucolytische geneesmiddel N-acetylcysteïne (NAC) zou mogelijk als behandeling voor acute TTP kunnen worden gebruikt omdat er al werd aangetoond dat het de VWF multimeergrootte reduceert.

Tijdens deze thesis werd de effectiviteit van NAC voor de preventie en genezing van acute TTP onderzocht met behulp van een muismodel voor congenitale TTP.

TTP werd geïnduceerd in $Adamts13^{-/-}$ muizen door injectie van 2000-2250 U/kg recombinant VWF (rVWF). In dit model werd 800 mg/kg NAC profylactisch (15 min voor rVWF injectie) of ter genezing van TTP (1 en 12 uur na rVWF injectie) toegediend. Bloed- en plasmastalen werden onderzocht op de aanwezigheid van TTP symptomen, zoals trombocytopenie, hemolytische anemie en weefselschade.

De profylactische toediening van NAC kon het onstaan van TTP symptomen in muizen vermijden. Vierentwintig uur na rVWF injectie waren zowel het bloedplaatjesaantal en de hemoglobine levels significant hoger in behandelde muizen dan in controle muizen, terwijl LDH activiteitslevels significant lager waren. Daarentegen was de toediening van NAC ter genezing van bestaande TTP symptomen niet effectief. NAC kon VWF in circulatie van beide muizengroepen die NAC toegediend kregen reduceren, maar VWF in bestaande bloedplaatjesaggregaten kon in vitro niet worden afgebroken.

NAC bleek effectief voor de preventie van TTP, maar niet voor de genezing van bestaande TTP symptomen in muizen.

List of Abbreviations

ADAMTS13	A Disintegrin-like And Metalloprotease with ThromboSpondin Type 1 repeats, member 13
AP	alkaline phosphatase
BSA	bovine serum albumin
C	cysteine-rich domain
C8	cysteine 8
CK	cystine-knot
CSP	cryosupernatant plasma
CTCK	C-terminal cystine-knot
CUB	Complement component C1r/C1s Urinary epidermal growth factor and Bone morphogenic protein 1 domains
D	disintegrin-like domain
E	fibronectin type-1 like
EDTA	ethylenediaminetetraacetic acid
ELISA	enzyme-linked immunosorbent assay
ER	endoplasmic reticulum
FDA	Food and Drug Administration
FFP	fresh frozen plasma
FVIII	coagulation factor VIII
GPIbalpha	platelet glycoprotein Ibalpha
GPIIb/IIIa	platelet glycoprotein Iib/IIIa
GSH	glutathione
Hb	hemoglobin
HMW	high molecular weight
HRP	horseradish peroxidase
HT	HEPES Tyrode
HUS	hemolytic uremic syndrome
IEF	isoelectric focusing
LDH	lactate dehydrogenase
LMW	low molecular weight
M	metalloprotease domain
MMW	medium molecular weight
NAC	N-acetylcysteine

NAPQI	N-acetyl-p-benzoquinone imine
NHP	normal human plasma
NMP	normal murine plasma
OPD	o-phenylenediamine
PBS	phosphate buffered saline
PBS-T	PBS with 0.1% Tween20
RAH	rabbit-anti-human
RGD	Arginine-Glycine-Aspartate
rGPIb	recombinant GPIb
ROS	reactive oxygen species
RT	room temperature
rVWF	recombinant human VWF
S	spacer domain
SDP	solvent/detergent-treated pooled plasma
SDS	sodium dodecyl sulphate
TBS	tris-buffered saline
TBS-T	TBS with 0.1% Tween20
TIL	trypsine inhibitor-like
tPA	tissue plasminogen activator
TSP-1	thrombospondin-1
TSR	thrombospondin type 1 repeat
TTP	thrombotic thrombocytopenic purpura
Uegf	Urinary epidermal growth factor
UK	United Kingdom
UL	ultra large
uPA	urokinase
USA	United States of America
USS	Upschaw-Schulman syndrome
VMA	Valine-Methionine-Alanine
VWA	von Willebrand A
VWC	von Willebrand C
VWD	von Willebrand D
VWF	von Willebrand factor
WPB	Weibel-Palade body

Contents

Part I

Literature review

Chapter 1

Hemostasis

Human blood is a complex fluid consisting of an aqueous fraction rich in proteins in which circulating blood cells are suspended. Three types of blood cells exist: red blood cells (erythrocytes), white blood cells (leukocytes) and blood platelets (thrombocytes) each having their own functions. Erythrocytes are the most abundant type of blood cells and transport oxygen from the lungs to tissues. Leukocytes are part of the body's immune system. Thrombocytes are small anuclear cell fragments that bud off from megakaryocytes and are very important in the process of hemostasis (Schulze and Shivdasani, 2005). This is the body's normal response that ceases bleeding at the site of an injury while maintaining normal blood flow elsewhere in the circulation. Hemostasis consists of three main processes. Primary hemostasis refers to the process where platelets adhere to the damaged or disrupted endothelium and to each other with subsequent forming of a platelet plug. This mechanism only takes place when vessels are injured, leading to the activation of platelets. Secondary hemostasis refers to the deposition of insoluble fibrin, which stabilizes the platelet aggregate. This is the result of a cascade of coagulation serine proteases. Thrombin is the central protease in the cascade and executes the conversion of soluble fibrinogen to insoluble fibrin. These two mechanisms lead to the formation of a fibrin- and platelet rich blood clot (Gale, 2011). The last stage is named fibrinolysis and results in the decomposition of the blood clot. This process occurs through the action of plasmin, which is a serine protease that degrades fibrin. This enzyme originates from plasminogen activation by either tissue plasminogen activator (tPA) or urokinase (uPA). Fibrinolysis is strictly regulated by several other activators and inhibitors (Chapin and Hajjar, 2015). Hemostatic abnormalities can lead to excessive bleeding or thrombosis.

Chapter 2

Von Willebrand factor

Von Willebrand factor (VWF) is a large multimeric glycoprotein with an important role in hemostasis and thrombosis. VWF is essential for the adhesion and aggregation of circulating platelets at sites of vascular injury. Besides this, VWF binds and transports coagulation factor VIII (FVIII) thereby protecting it from rapid degradation, cellular uptake and binding to the surface of activated platelets and endothelial cells. VWF is also involved in several pathologic processes beyond hemostasis including angiogenesis, cell proliferation, inflammation and tumor cell survival and metastasis (Luo et al., 2012; Lenting et al., 2012; Zhou et al., 2012). Quantitative or qualitative abnormalities in VWF give rise to a hereditary severe bleeding tendency, known as von Willebrand disease (VWD). This disease was first described by Erich von Willebrand in 1926 (Lenting et al., 2012). In addition, VWF is associated with many other disorders including thrombotic thrombocytopenic purpura (TTP), various vascular disorders and liver diseases (Luo et al., 2012).

2.1   Biosynthesis and secretion

VWF is encoded on the short arm of chromosome 12 and comprises 52 exons (Hernandez-Zamora et al., 2015). The protein is synthesized as pre-pro-VWF, which consists of a signal peptide, propeptide and mature multidomain subunit. The synthesis is confined to the endothelial cells and megakaryocytes (Crawley et al., 2011). The biosynthesis of VWF is a complex process including the removal of the signal- and propeptide, extensive O- and N-linked glycosylation, sulphatation and multimerization (Crawley et al., 2011; Luo et al., 2012; De Meyer et al., 2009). The signal peptide ensures the translocation of pre-pro-VWF to the endoplasmic reticulum (ER). There, multimerization of VWF starts with the formation of dimers. Cysteine residues in the cystine-knot (CK) domain form intermolecular disulphide bonds ('tail-to-tail' association). The actual multimerization of the dimers occurs in the Golgi apparatus. Domains D1 and D2, forming the propeptide, catalyse this process by acting as a protein disulphide isomerase. The N-termini of VWF dimers are thereby disulphide-linked ('head-to-head' association). After the multimerization and glycosylation of VWF, the propeptide

is removed by the enzyme furin (Figure 2.1). VWF is subsequently transported to Weibel-Palade bodies (WPBs) of the endothelial cells or α-granules of platelets, both acting as storage organelles for ultra large (UL)-VWF (Crawley et al., 2011). The secretion of VWF from endothelial cells occurs via two distinct pathways. The constitutive pathway links secretion directly to synthesis. In the regulated pathway, VWF is released from the storage organelles after a physiological agonist promotes the secretion. VWF originating from α-granules is only derived via the regulated pathway. Therefore, VWF in circulation mainly originates from endothelial cells, as platelets only release their α-granule content when activated (Crawley et al., 2011, Ruggeri, 2007).
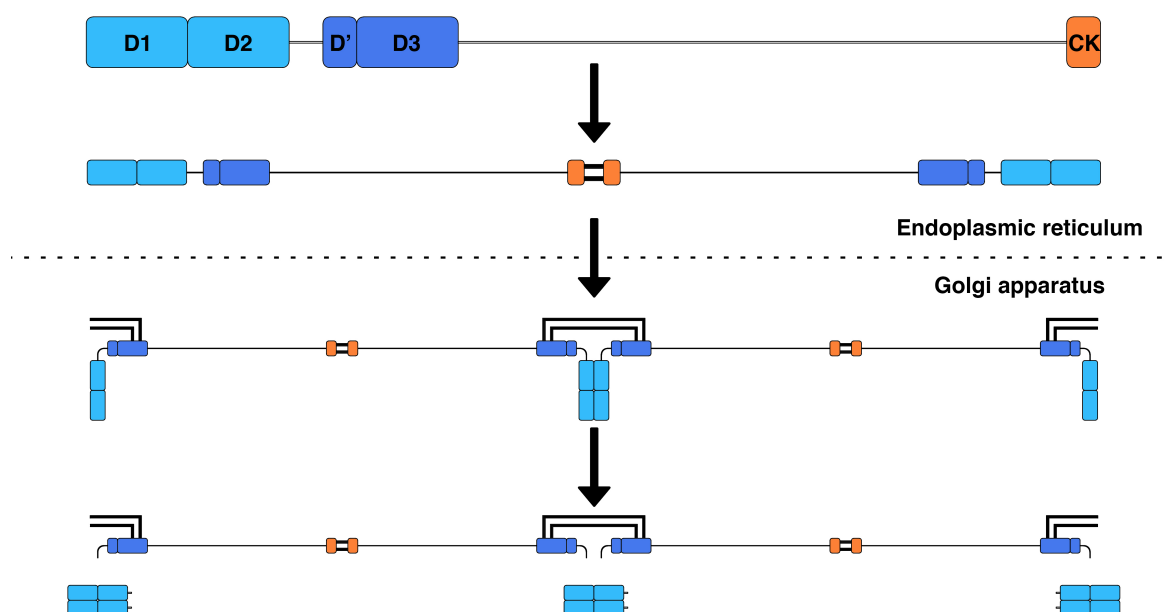
Figure 2.1: The assembly of VWF multimers. In the ER, the multimerization of VWF starts with the formation of dimers. Cysteine residues in the CK domain form intermolecular disulphide bonds, this is called the 'tail-to-tail' association. The actual multimerization of the dimers occurs in the golgi apparatus. The propeptide catalyses this process by acting as a protein disulphide isomerase. The N-termini of the VWF dimers become disulphide-linked, forming the proVWF multimers. This process is named 'head-to-head' association. Afterwards, the propeptide is removed by furin and VWF is transported to the WPBs of endothelial cells or α-granules of platelets (Sadler, 2005).

2.2 Multidomain structure

The multimeric VWF protein consists of a variable number of identical, covalently linked subunits of approximately 250 kDa. Each mature monomer consists of 2050 amino acid residues and has a multidomain structure consisting of following domains: D1-D2-D'-D3-A1-A2-A3-A4-D4-C1-C2-C3-C4-C5-C6-CK (Figure 2.2) (Ruggeri, 2007; Zhou et al., 2012).
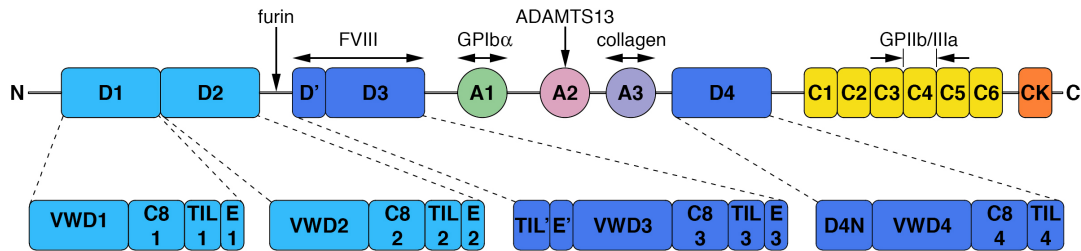
Figure 2.2: The structure of VWF. VWF consists of a signal peptide, a propeptide and the mature multidomain subunit. The N-terminal signal peptide ensures the translocation of pre-pro-VWF to the ER. The propeptide is composed of the D1 and D2 domains and is removed by the enzyme furin. The D'-D3 domain is responsible for the binding of FVIII, thereby elongating its half-life in the bloodstream. The A1 domain contains the platelet GPIbα binding site. The Y1605-M1606 ADAMTS13 cleavage site is situated within the A2 domain of VWF. The A3 domain binds subendothelial collagen. The C4 domain contains the RGD sequence. This sequence is recognized by the platelet integrin GPIIb/IIIa. The CK domain is important in the formation of VWF dimers by 'tail-to-tail' associations. VWF also contains C1, C2, C3, C5, C6 domains. The subdomains of the different D domains are also depicted (Crawley et al., 2011; Zhou et al., 2012).

2.2.1 VWA domains

The three von Willebrand A (VWA) domains, A1, A2 and A3 are large and globular, containing hydrophobic cores (Zhou et al., 2012). These three domains are very homologous (Figure 2.3). The A1 and A3 domains contain an intradomain disulphide bond, which couples the N- and C-terminus. The A2 domain lacks this bond, but contains a vicinal disulphide bond at the C-terminus. In this domain, one of the amphipathic α-helices is substituted by a less-ordered loop. These two characteristics make the A2 domain more susceptible to unfolding than the A1 and A3 domain. The three domains possess important binding- and cleavage sites, which are essential for

the hemostatic function of VWF (Zhang et al., 2009). One of the main functions of VWF is the tethering of platelets. The binding site for platelet glycoprotein Ibα (GPIbα) is located within the A1 domain of VWF. GPIbα is a component of the platelet glycoprotein Ib/IX/V receptor complex (Crawley et al., 2011; Ruggeri, 2007). The initial multimeric VWF secreted from endothelial cells is ultra large in size and therefore prothrombotic. The metalloprotease ADAMTS13 (A Disintegrin-like And Metalloprotease with ThromboSpondin Type 1 repeats, member 13), controls the size of prothrombotic UL-VWF by cleavage of Y1605-M1606. This peptide bond is situated within the A2 domain of VWF (Crawley et al., 2011). Subendothelial collagen is exposed to the lumen of the blood vessel after blood vessel damage. This collagen is recognized and binds the A3 (and A1) domain of VWF. The collagen binding site located within the A3 domain of VWF is exposed in globular and elongated VWF. On the other hand, the GPIbα binding site within A1 and the ADAMTS13 cleavage site within A2 are only exposed in the elongated form of VWF (Crawley et al., 2011). In the folded form, the platelet binding site within the A1 domain is masked by the N-terminal D'D3 domain and the C-terminal part of A2. The ADAMTS13 cleavage site is buried inside the folded A2 domain. Therefore, the globular, folded conformation of VWF inhibits both platelet adhesion and proteolysis at the ADAMTS13 cleavage site (Ulrichts et al., 2006; Nishio et al., 2004; Crawley et al., 2011).
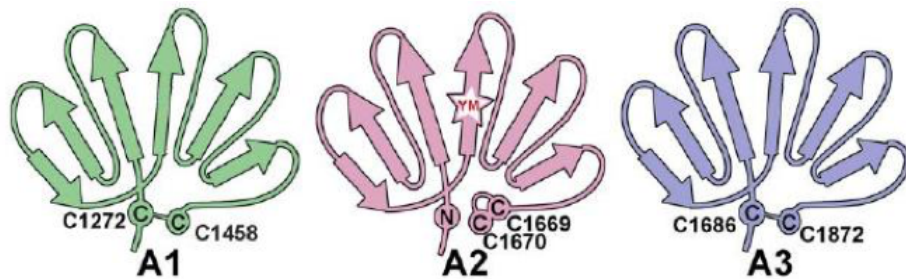
Figure 2.3: The schematic representation of the VWF A1, A2 and A3 domains. The VWF A1, A2 and A3 domains are structural homologous. The A1 and A3 domain are characterized by an intradomain disulphide bond, which couples the N- and C-terminus. The A2 domain contains a vicinal disulphide bond at the C-terminus and the Y1605-M1606 ADAMTS13 cleavage site (Crawley et al., 2011).

2.2.2 VWF D domains

The different D domains of VWF are divided into multiple subdomains. These D domains are composed of the smaller modules von Willebrand D (VWD), 8-cysteine (C8), trypsine inhibitor-like (TIL), fibronectin type-1 like (E) and D4N. The D1 domain is composed of the subdomains VWD1, C8-1, TIL-1 and E-1. The D2 domain is an assembly of the modules VWD2, C8-2, TIL-2 and E-2. These two domains together form the propeptide of VWF and promote the 'head-to-head' association of VWF dimers. The D'D3 domain of VWF consists of the TIL', E', VWD3, C8-3, TIL-3, E-3 subdomains. This domain is responsible for the binding of FVIII, thereby elongating its half-life in the bloodstream. The last D domain, D4, contains a unique D4N module. The domain is composed of the D4N, VWD4, C8-4 and TIL-4 modules (Figure 2.2) (Zhou et al., 2012).

2.2.3 VWC domains

The former prediction of the multidomain structure of VWF, D1-D2-D'-D3-A1-A2-A3-A4-D4-B1-B2-B3-C1-C2-CK, is re-annotated and consists now of six tandem von Willebrand C (VWC) and VWC-like domains with a highly extended conformation. The C1, C3 and C5 are VWC domains and the intervening C2, C4 and C6 are VWC-like domains, which are similar in length and sequence to the VWC domains. Each VWC module is subdivided into two extended, highly flexible, disulphide-linked subdomains. The VWC domains offer flexibility and extend the length of VWF. The C4 domain contains the Arginine-Glycine-Aspartate (RGD) sequence. This sequence is recognized by the platelet integrin $\alpha_{IIb}\beta_3$, also known as platelet glycoprotein IIb/IIIa (GPIIb/IIIa) (Zhou et al., 2012).

2.2.4 CTCK domain

Cystine-knot (CK) domains are found in various proteins. Alike VWF, Norrie disease protein, mucins and connective tissue growth factor are C-terminal cystine-knot (CTCK) containing proteins (Zhou et al., 2012). The common structural core of CK containing proteins is formed by a pattern of three disulphide bridges. One disulphide bridge passes between the centre of a ring formed by the two other disulphide bridges (Meitinger et al., 1993). Other cysteine-residues in the CTCK domain mediate the dimerization of VWF monomers.

2.3   Functionality

The action of VWF is dependent on both its conformation and its size. The larger VWF multimers comprise more platelet- and collagen binding sites. In addition, they are more prone to vascular shear forces, which in turn leads to a higher exposure of the ligand binding sites. This makes these larger multimers more hemostatically reactive than the smaller forms (Sadler 1998). The main regulator of VWF multimer size is the metalloprotease ADAMTS13. As mentioned above, the ADAMTS13 cleavage site and the platelet GPIbα binding site are only exposed in the elongated form. An elevated shear force in the bloodstream causes a conformational change from the globular to the elongated form. Three different locations where VWF is prone to cleavage by ADAMTS13 can be distinguished: First, this can occur when the VWF A3 domain binds a subendothelial collagen-rich matrix, which is exposed after vessel damage. The cryptic platelet binding sites (in the A1 domain) become exposed and are able to recruit circulating platelets to the site of vascular damage. Furthermore, the VWF scissile bonds (in the A2 domain) become accessible for cleavage by ADAMTS13, thereby reducing the VWF multimer size (Crawley et al., 2011). Second, elevated vascular shear forces are present on the portion of secreted UL-VWF that stays attached to the endothelium. VWF becomes unravelled and is prone to cleavage by ADAMTS13. Subsequently, smaller VWF strings are released in the bloodstream and adapt the globular form (Dong et al., 2002). Third, globular UL-VWF exposes its scissile bond when passing through the microvasculature. This again results in smaller, less reactive VWF multimers. The conformation- and size dependent mechanism of VWF cleavage allows the prevention of unnecessary and spontaneous thrombus formation (Crawley et al., 2011).

In addition to ADAMTS13, other proteins exist that regulate VWF multimer size. In vitro, plasma VWF can also be cleaved by other proteases including leukocyte protease proteinase 3, cathepsin G, elastase and granzyme B. (De Ceunynck et al., 2013). Thrombospondin-1 (TSP-1) is another example of a protein that can regulate VWF multimer size. TSP-1 is present in the α-granules of platelets and it is released when platelets are activated. When TSP-1 is present, the average multimer size of plasma VWF is significantly larger. This is due to a competition between the binding of ADAMTS13 and TSP-1 for their binding sites in the VWF A2-A3 domains. Therefore, ADAMTS13 is unable to cleave VWF when TSP-1 is bound to VWF (Pimanda et al., 2004; Wang et al., 2010).

Chapter 3

ADAMTS13

The von Willebrand factor-cleaving protease was identified in 2001 as ADAMTS13 (Levy et al., 2001). This enzyme controls thrombus formation through the cleavage of UL-VWF via the Y1605-M1606 peptide bond (or Y842 - M843, numbering of the protein sequence). These smaller VWF multimers travel through blood vessels without being excessively cleaved and without binding of platelets. A congenital or acquired deficiency of the plasma protease can cause the disease thrombotic thrombocytopenic purpura (TTP). VWF is the only known substrate of ADAMTS13. The ADAMTS13 gene maps to chromosome 9q34 and is composed of 29 exons (Levy et al., 2001). The enzyme is primarily derived from hepatic stellate cells. However, ADAMTS13 may also be expressed in lower levels by renal podocytes and tubular cells, vascular endothelial cells and megakaryocytes/platelets (Tsai, 2010). ADAMTS13 is present in plasma at a concentration of 1 μg/mL and has an elimination half-life of about two days in circulation (Tsai, 2010; Moake, 2002; Feys et al., 2006). ADAMTS13 can be proteolytic inactivated by the coagulation proteases plasmin and thrombin. This may play a role in controlling the activity of ADAMTS13, but it remains uncertain if this is a pathological phenomenon or a normal control mechanism (Crawley et al., 2005; Feys et al., 2010a).

3.1   Multidomain structure

Human ADAMTS13 is a member of the ADAMTS family, which are Zn^{2+}-dependent metalloproteases. ADAMTS13 has a molecular weight of approximately 180 kDa and is composed of 1427 amino acid residues (Crawley et al., 2011; Zheng et al., 2001). The metalloprotease consists of a multidomain structure including a signal peptide, short propeptide, metalloprotease domain (M), disintegrin-like domain (D), thrombospondin type 1 repeat (TSR 1), cysteine-rich domain (C), spacer domain (S), seven additional TSRs (TSR 2-8) and two Complement component C1r/C1s, Urinary epidermal growth factor (Uegf), and Bone morphogenic protein 1 domains (CUB).

The N-terminal part of ADAMTS13 consists of the M, D, TSR 1, C and S domains, therefore this part of the enzyme is called MDTCS. The C-terminal part is named T2-CUB2 and consists of seven TSRs (TSR 2-8) and the two CUB domains (Figure 3.1) (Tsai, 2010; Crawley et al., 2011; Zheng et al., 2001).
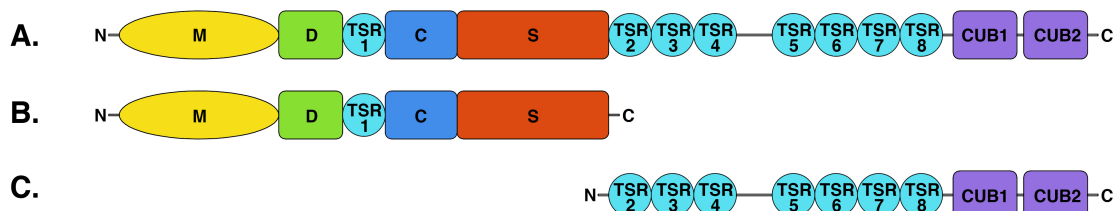
Figure 3.1: The structure of ADAMTS13. (A) ADAMTS13 is composed of a metalloprotease domain (M), disintegrin-like domain (D), thrombospondin type 1 repeat (TSR 1), cysteine-rich domain (C), spacer domain (S), seven additional TSRs (TSR 2-8) and two CUB domains. (B) The N-terminal part of ADAMTS13 consists of the M, D, TSR 1, C and S domains, therefore this part of the enzyme is called MDTCS. (C) The C-terminal part is named T2-CUB2 and consists of seven TSRs (TSR 2-8) and the two CUB domains (Crawley et al., 2011).

3.2   Metalloprotease domain

The metalloprotease domain contains the active site of the enzyme. Just as the other members of the ADAMTS family, the metalloprotease domain is characterized by a reprolysin-type Zn^{2+}- binding structure: HEXXHXXGXXH. This motif contains three highly conserved Zn^{2+}- binding histidine residues (His224, His228 and His234) and a catalytic glutamate residue (Glu225). Together with the bound Zn^{2+} ion, this glutamate residue polarizes a water molecule and is therefore part of the proteolytic machinery (de Groot et al., 2010; Crawley et al., 2011). The Zn^{2+}-binding motif is followed by a Met-turn, which contains a methionine residue located in the conserved Valine-Methionine-Alanine (VMA) sequence (Somerville et al., 2003). Besides Zn^{2+}, ADAMTS13 needs Ca^{2+} for its proteolytic activity. This cation is present in a loop adjacent to the active site and is probably important in preserving the secondary structure of the metalloprotease domain (Gardner et al., 2009). Next to the proteolytic function of the M domain, it interacts with VWF residues in the vicinity of the cleavage site. The aromatic side chain of the VWF P1 residue (Y1605) is required for normal functioning of ADAMTS13. This residue is accommodated in the corresponding ADAMTS13 S1 binding pocket (including residues L151 and V195). The VWF

P1' residue is a large, hydrophobic amino acid (M1606), which is also important for normal proteolysis. P1' is adapted in its complementary ADAMTS13 binding pocket S1' (including residues D252- P256). ADAMTS13 also binds VWF N-terminally to the cleavage site. The VWF P3 residue (L1603) and to a minor extent the VWF P2 residue (V1604) are involved in this interaction (Crawley et al., 2011).

3.2.1 Disintegrin-like domain

The disintegrin-like domain doesn't seem to operate like a distintegrin protein. Instead, it shares more structural characteristics with the cysteine-rich domain (Crawley et al., 2011). The D domain is proposed to be important for both ADAMTS13 enzyme activity and specificity. Residues R349 and L350 of the D domain can make interactions with D1614 and A1612 of VWF respectively. These interactions support the positioning of the VWF scissile bond near the ADAMTS13 active site cleft (de Groot et al., 2009).

3.2.2 Thrombospondin type 1 repeats

ADAMTS13 contains eight thrombospondin type 1 repeats. One TSR is situated between the D and C domain and is very analogous in all ADAMTS family members, generally comprising six cysteine residues. The seven additional TSRs are located between the S and first CUB domain and are considerably more variable in sequence. The TSRs display homology to the type 1 repeat of the proteins thrombospondin-1 and -2 (group A thrombospondins), which are both potent inhibitors of angiogenesis (Crawley et al., 2011).

3.2.3 Cysteine-rich domain

The cysteine-rich domain is highly conserved among ADAMTS family members, which almost all comprise ten conserved cysteine residues (Crawley et al., 2011). The region spanning residues F502 to C555 is the most conserved region, suggesting a structural role for this element in ADAMTS proteins. The non-conserved region in the C domain comprises residues A451 to S501, indicating its possible enzyme-specific function. Hydrophobic residues in both the non-conserved region of the ADAMTS13 C domain and in VWF are suggested to be important for proteolysis (de Groot et al., 2015).

3.2.4   Spacer domain

The spacer domain is a long segment without cysteine residues. The domain folds into a single globular domain consisting of ten antiparallel β-strands. These strands are organized in a jelly-roll topology, forming two antiparallel β-sheets. This domain shows the least homology with spacer regions of other ADAMTS family members (Akiyama et al., 2009). After (partial) unfolding of the VWF A2 domain, a cryptic exosite on the C-terminal part of VWF A2 (E1160- R1668) becomes available for binding by residues of the spacer domain. This enhances the affinity of ADAMTS13 for VWF (Crawley et al., 2011).

3.2.5   CUB domains

Members of the ADAMTS family have a large variety in C-terminal domains. ADAM-TS13 is the only one that possesses CUB domains. Other known proteins that contain the CUB-module are important for developmental regulation, like the bone morphogenetic protein-1 and the dorso-ventral patterning protein tolloid (Bork and Beckmann, 1993).

3.3   Mode-of-action

The proteolysis of the VWF scissile bond by ADAMTS13 is dependent on the interaction of multiple domains and involves conformational changes. The circulating globular form of VWF is bound by ADAMTS13. This interaction involves the ADAMTS13 TSR 5-8 and CUB domains and the VWF D4-CK domains (Figure 3.2 A). In plasma, a fraction of the circulating ADAMTS13 ($\pm$ 3%) and globular VWF are in complex with each other (Feyst et al., 2009). By means of this interaction, ADAMTS13 can be incorporated in a thrombus together with VWF (Crawley et al., 2011; Feys et al., 2009). When elevated shear forces act upon VWF, the A2 domain will become unfolded (Figure 3.2 B). This reveals additional binding sites on VWF for complementary sites on ADAMTS13. First, residues in the ADAMTS13 spacer domain interact with the C-terminal part of the VWF A2 domain (Figure 3.2 C). Subsequently, a critical (low affinity) interaction between the ADAMTS13 disintegrin-like domain and a domain adjacent to the VWF scissile bond helps to approximate and to position the cleavage site (Figure 3.2 D). Thereafter, the metalloprotease domain interacts with VWF N-terminally to the scissile bond (Figure 3.2 E). Finally, the metalloprotease domain binds the Y1605-M1606 cleavage site, leading to proteolysis (Figure 3.2 F)

(Crawley et al., 2011). According to this model, the activity of ADAMTS13 is regulated by the conformation of the substrate VWF.

It was recently shown that the activity of ADAMTS13 is also controlled by the conformation of the enzyme itself (South et al., 2014; Muia et al., 2014; Deforche et al., 2015). It was proposed that ADAMTS13 in circulation is present in a closed conformation due to the interaction of the CUB domains with the spacer domain, preventing the enzyme from interacting efficaciously with its binding site in the VWF A2 domain. The CUB-spacer interaction is interrupted when ADAMTS13 binds the C-terminal domains of VWF. This results in a conformational activation of the enzyme (South et al., 2014; Muia et al., 2014; Deforche et al., 2015).
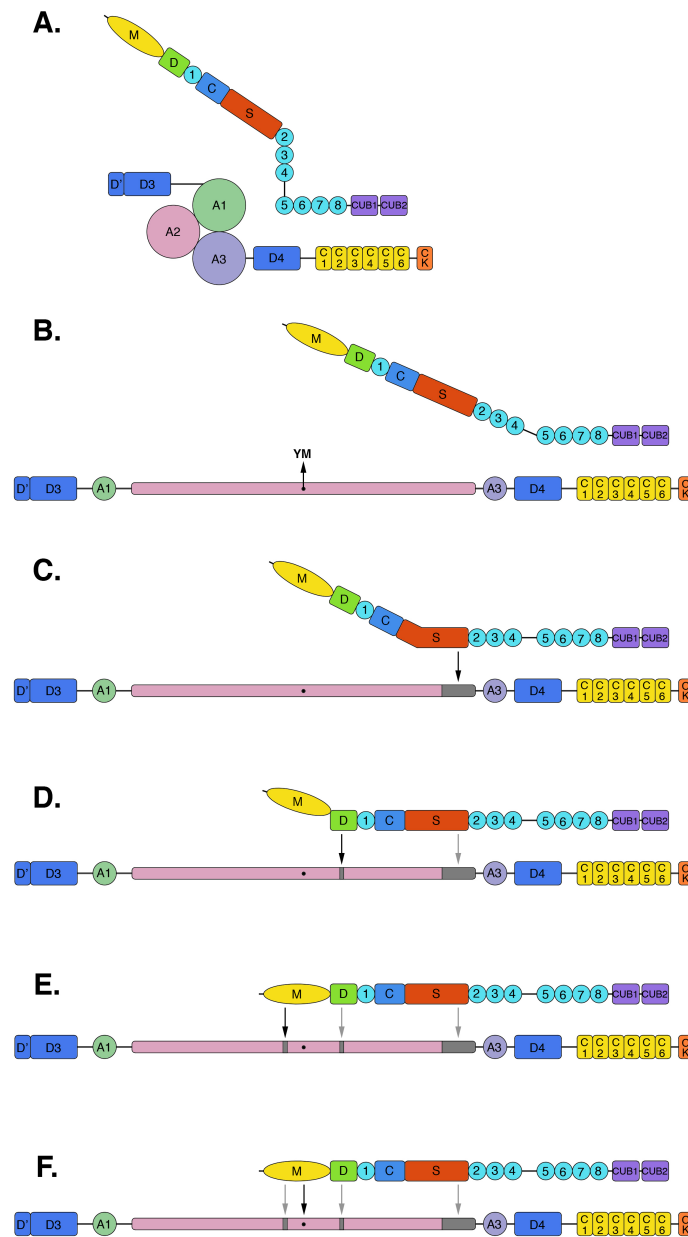
Figure 3.2: The proteolysis of VWF by ADAMTS13. (A) Globular VWF in circulation is bound by ADAMTS13. This interaction involves the ADAMTS13 TSR 5-8 and CUB domains and the VWF D4-CK domains. (B) Upon elevated shear stress, the A2 domain of VWF will become unfolded. (C) Residues in the ADAMTS13 spacer domain interact with the C-terminal part of the VWF A2 domain. (D) A critical, but low affinity interaction between the ADAMTS13 disintegrin-like domain and an area adjacent to the scissile bond takes place. (E) The metalloprotease domain interacts with VWF N-terminally to the scissile bond. (F) The metalloprotease domain binds the Y1605-M1606 cleavage site, leading to proteolysis (Crawley et al., 2011).

Chapter 4

Thrombotic thrombocytopenic purpura

Thrombotic thrombocytopenic purpura (TTP) is a rare and life-threatening microangiopathic disease with an annual incidence of four cases per million people. TTP occurs more in women and usually appears in the fourth decade of life (Coppo and Veyradier, 2012). The disease is characterized by VWF- and platelet-rich microthrombi in terminal arterioles and capillaries of vital organs (often heart, kidney and brain), which ultimately results in organ dysfunction. Because of the accumulation of platelets in these thrombi, they are depleted in the blood, causing thrombocytopenia. Thrombocytopenia causes the formation of red-purple dots under the skin, named purpura, as a result of internal hemorrhage of the vascular wall (Figure 4.1a). TTP patients also suffer from hemolytic anemia, because of the presence of fragmented red blood cells (schistocytes) (Figure 4.1b). The pathophysiology of TTP can be partially explained by the deficiency of the VWF-cleaving protease ADAMTS13. When ADAMTS13 is absent or dysfunctional, UL-VWF multimers cannot be cleaved, are hyperreactive and can cause the formation of microvascular occlusions by spontaneous adhesion of platelets (Moake, 2002). However, a relevant number of TTP patients may display a moderate reduced or normal VWF-cleaving activity. Additional genetic- or environmental triggers are often necessary to induce acute TTP episodes.

(a)   (b)
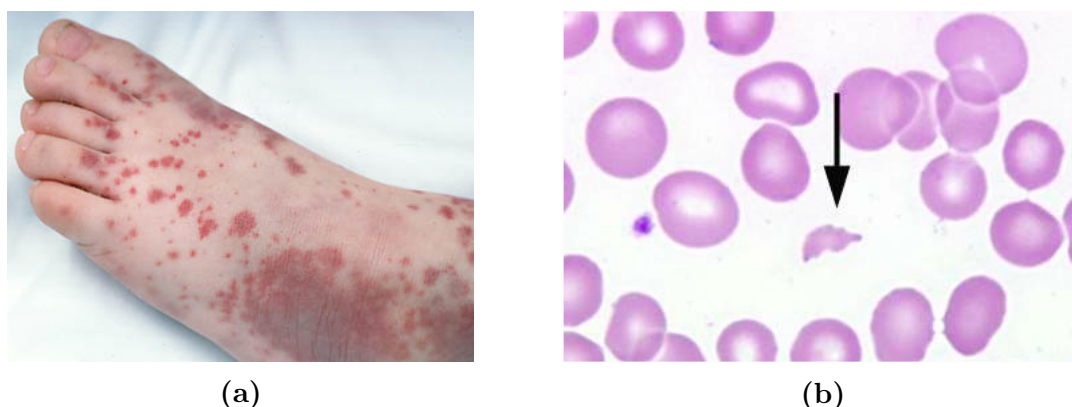
Figure 4.1: Characteristics of TTP. TTP is characterized by VWF- and platelet-rich microthrombi, thrombocytopenia which can result in red-purple dots under the skin (purpura, left picture) and fragmented red blood cells (schistocytes, right picture).

4.1   Congenital and acquired TTP

The deficiency of the plasma metalloprotease ADAMTS13 in TTP patients can be caused by mutations in the ADAMTS13 gene. However in most cases, autoantibodies against the enzyme are found in the plasma of acquired TTP patients. Discrimination between both forms is important for the therapeutic management of an acute TTP episode.

4.1.1   Congenital TTP

The hereditary or congenital form of TTP, also known as the Upshaw-Schulman syndrome (USS), is an extremely rare disorder. It represents about less than five percent of the TTP patients (Vanhoorelbeke and De Meyer, 2013). However, it is believed that USS may have been remarkably underestimated and misdiagnosed. Although congenital TTP patients have a severe ADAMTS13 deficiency, they are not continuously suffering from acute TTP episodes. This indicates that additional triggers are needed to induce an acute TTP event (Lammle et al., 2005). About half of the USS patients present their first acute TTP bout within their first five years of life (early onset TTP). The other patients seem to remain asymptomatic until 20 to 40 years of age. A few patients are even asymptomatic until they are more than 60 years of age (late onset TTP) (Hovinga and Lammle, 2012).

The disease results from homozygous or compound heterozygous mutations in each of the two 9q34 ADAMTS13 alleles. Heterozygous carriers are constantly asymptomatic (Lammle et al., 2005). There are over 140 mutations identified including missense mutations, small deletions or insertions, nonsense mutations and splice site mutations (Tsai, 2010). The affected residues span across the entire spectrum of the gene resulting in an impaired protein synthesis, secretion or proteolytic activity. Thus far, no link has been established between the ADAMTS13 genotype and the clinical phenotype (Tsai, 2010).

4.1.2   Acquired idiopathic TTP

The acquired form of TTP results from circulating anti-ADAMTS13 autoantibodies. In the majority of these patients, inhibitory antibodies are present which block the proteolytic activity of ADAMTS13 towards VWF. Besides the inhibitory antibodies, non-inhibitory ADAMTS13 antibodies also exist. These probably enhance the clear-

ance of ADAMTS13 from the circulation or they may interfere with the interaction of ADAMTS13 with cells or other plasma proteins than VWF (Scheiflinger et al., 2003). Anti-ADAMTS13 antibody titers vary considerably among patients, ranging from less than 100 ng/mL to more than 1 µg/mL (Luken et al., 2005).

Antibody epitopes

Multiple domains of ADAMTS13 are recognized by autoantibodies from acquired TTP patients. The majority of these patients possess antibodies targeting the cysteine-rich or spacer domain of ADAMTS13. Most of these patients also have antibodies directed against the C-terminal half of the enzyme (TSR 2-8 and/or CUB domains) (Luken et al., 2005; Zheng et al., 2010). The main mechanism of action of anti-C-terminal antibodies is thought to be via an increased clearance of the antigen ADAMTS13. The inhibitory antibodies are limited to the anti-spacer/cysteine-rich domain antibodies (Thomas et al., 2015).

Antibody (sub)class distribution

The antibodies are predominantly members of the immunoglobulin (Ig)G class, but IgA en IgM anti-ADAMTS13 antibodies are also detected (Ferrari et al., 2007). Members of the various Ig (sub)classes differ in their biological functions. They exhibit different capacities to bind to cell surface Fcγ receptors or to activate complement proteins. Therefore they mediate different immunologic effector functions (Ferrari et al., 2009).

IgG4 (either alone or in association with other IgG subclasses) is the most common IgG subclass in TTP patients, followed by IgG1. These subclasses exhibit an inverse correlation of antibody titers. Patients with high levels of IgG4 (and thereby low IgG1 levels) are believed to be more prone to relapse than patients with low IgG4 levels (and thereby high IgG1 levels) (Ferrari et al., 2009). However, higher levels of IgG4 in acquired TTP patients are believed to characterize a more treatable form of the disease (Ferrari et al., 2009). Subclasses IgG2 and IgG3 are less represented in this autoimmune disorder (Ferrari et al., 2009).

4.1.3   Secondary TTP

Non-idiopathic or secondary TTP can occur in association with HIV infection, connective tissue diseases, pregnancy, cancer, bone marrow transplantations and after

treatment with antiplatelet agents such as clopidogrel and ticlopidine. Unlike congenital and idiopathic TTP, severe ADAMTS13 deficiency is extremely rare in secondary forms of TTP (Coppo and Veyradier, 2012).

4.2 Diagnosis and therapy

4.2.1 Diagnosis

TTP is difficult to diagnose as overlapping symptoms are found in other microangiopathic diseases, like the hemolytic uremic syndrome (HUS). Historically, TTP was defined as the classic pentad of symptoms including microangiopathic hemolytic anemia, peripheral thrombocytopenia, fever, neurological symptoms and renal failure (Sadler, 2008). However, not all of the TTP patients exhibit those five symptoms. Because of the need for a rapid diagnosis of the disease to start the correct treatment in time, a decrease in the stringency of the diagnostic criteria is required. Accordingly, the association of microangiopathic hemolytic anemia and thrombocytopenia should be sufficient to suggest the diagnosis of TTP (Blombery and Scully, 2014). ADAMTS13 assays may also help to confirm the diagnosis and to provide helpful guidelines for treatment. Other investigations that could be done are for example blood smear analysis, determining lactate dehydrogenase (LDH) activity and haptoglobin- and bilirubin-level measurements. The identification of congenital TTP cases is done by familial inquiry and genetic analysis. This is recommended when plasma infusion alone is sufficient to achieve remission and when ADAMTS13 autoantibodies are undetectable (Coppo and Veyradier, 2012; Blombery and Scully, 2014).

4.2.2 Therapy

The primary and most important treatment of acquired TTP is the use of plasma exchange therapy (PEX). PEX removes ADAMTS13 autoantibodies and restores ADAMTS13 activity in acquired TTP patients. For this therapy, cryosupernatant plasma (CSP), fresh frozen plasma (FFP) or solvent/detergent-treated pooled plasma (SDP) can be used, each having their own advantages and disadvantages. For instance, CSP contains lower UL-VWF levels and the action of SDP provides inactivation of lipid-enveloped viruses. The latter is also available as prion-reduced SDP (Blombery and Scully, 2014). Congenital TTP patients are treated with plasma infusion alone, because no antibodies have to be removed from circulation. Although the plasma half-life of ADAMTS13 is about two days, prophylactic plasma infusion is administered only

every two to three weeks to congenital TTP patients who are susceptible to relapses. It is not clear why the effect on platelet count lasts for up to three weeks (Lammle et al, 2005). Besides PEX, some acquired TTP patients are also treated with immunosuppressive therapy, including (cortico)steroids like prednisone and (methyl)prednisolone. Rituximab, another immunosuppressive component, is a chimeric monoclonal antibody against CD20 on B cells and is used for the treatment of refractory disease or relapses. It has been shown to decrease the amount of PEX to attain remission, to decrease the length of hospitalisation and to reduce the risk of relapse (Scully et al., 2011). Other immunomodulating medications that are sometimes given to TTP patients are mycophelolate, mofetil, cyclosporine and vincristine (Blombery and Scully, 2014). Another intervention that is occasionally done in relapsing acquired TTP patients is a splenectomy, which is preferably performed during remission. This decreases the autoantibody production, but has the consequence that an important source of B cells is turned off. Immunosuppressive therapeutics are not administered to congenital TTP patients, as they don't possess ADAMTS13 autoantibodies (Coppo and Veyradier, 2012; Blombery and Scully, 2014).

Although the use of plasma exchange or infusion has reduced the mortality rate from more than 90 percent to less than 20 percent, plasma therapy remains inconvenient, expensive and can cause various minor or major complications such as haemorrhage, sepsis, cardiac arrest and death (George, 2010). Future directions for new treatments of TTP target various aspects of the disease. The use of recombinant ADAMTS13 as a potential substitute for human plasma is tested in vitro and in vivo in mice and rats. In mice, the prophylactic administration of recombinant ADAMTS13 protected *Adamts13* knockout mice from TTP development. The effect of the therapeutic administration of recombinant ADAMTS13 was dependent on the time span after triggering TTP in *Adamts13* knockout mice (Schiviz et al., 2012). In vitro, it is able to overcome the ADAMTS13 autoantibodies and restores ADAMTS13 activity in human plasma samples (Plaimauer et al., 2011). This was confirmed in vivo where recombinant ADAMTS13 also prevents TTP symptoms in rats with acquired TTP-like symptoms (Tersteeg et al., 2015). Another possible mechanism for the treatment of TTP is the use of inhibitors for the VWF-GPIbα interaction. The aptamer (a nucleic acid macromolecule) ARC1779 binds to the A1 domain of VWF and subsequently blocks the interaction with platelet GPIbα (Cataland et al., 2012). The use of the Nanobody ALX-0081 (caplacizumab) or monoclonal antibody GBR600 was also able to inhibit

this interaction in baboons, reducing TTP symptoms (Ulrichts et al., 2011; Callewaert et al., 2012; Feys et al., 2012). In addition, Peyvandi et al. (2016) investigated the potential of caplacizumab for treating an acute episode of acquired TTP in a phase 2 clinical trial. In this study, 36 patients received caplacizumab daily in addition to standard treatment (PEX combined with immunosuppressive therapy) and the administration of the drug was continued for 30 days after the last plasma exchange. Further platelet aggregation was prevented more rapidly in these patients and consequently, TTP symptoms were resolved faster compared to patients receiving a placebo in addition to standard treatment.

4.2.3 NAC

The FDA-approved drug N-acetylcysteine (NAC) is used for the treatment of chronic congestive and obstructive lung diseases as well as in the case of acetaminophen (paracetamol) toxicity. N-acetyl-p-benzoquinone imine (NAPQI) is a metabolite of acetaminophen and is extremely toxic to the liver. Normally, NAPQI is detoxified by glutathione (GSH) but in case of an overdose acetaminophen, GSH is depleted. NAC prevents hepatic toxicity by restoring GSH levels in the liver (Heard, 2008). In the treatment of lung diseases, NAC functions as a mucolytic agent. NAC is composed of an L-cysteine residue with an acetyl moiety attached to the amine group (Figure 4.2). The mucolytic function is achieved by the free thiol group in the molecule, that is able to reduce disulphide bonds. This reduction in mucin multimer size decreases its viscosity and hence improves its clearance from the airways (Sheffner et al., 1964).
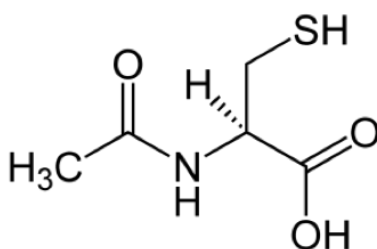
Figure 4.2: The structure of N-acetylcysteine. NAC is an acetylated L-cysteine residue. The free thiol group in the molecule functions as a reducing agent.

VWF polymerizes in a similar manner as mucin multimers, i.e. forming dimers in the ER and multimers in the golgi-apparatus. Therefore, it was proposed that NAC could also reduce VWF multimers. Chen et al. showed that NAC reduces VWF-multimer size in vitro and in mice in a concentration-dependent manner. Besides this, they demonstrated that NAC inhibits VWF-dependent platelet aggregation and collagen binding which both correlate with VWF multimer size. In addition, they showed that before the VWF interchain disulphide bonds are reduced, the intrachain disulphide bond Cys1272-Cys1458, required for platelet binding to the VWF A1 domain, is reduced. These results suggests that NAC may be a promising therapeutic agent for TTP (Chen et al., 2011).

Preliminary case reports however demonstrate varying outcomes on the effectiveness of this therapy in TTP patients (Chapin et al., 2012; Li et al., 2014; Shortt et al., 2013; Shortt et al., 2014; Rottenstreich et al., 2015; Cabanillas and Popescu-Martinez, 2015). In the case studies of Chapin et al. (2012) and Shortt et al. (2013), two patients suffering from severe TTP symptoms failed to respond to NAC treatment in addition to standard plasma exchange- and immunosuppressive therapy. In the studies of Li et al. (2014) and Rottenstreich et al. (2015), four TTP patients were succesfully treated with NAC in addition to standard therapy, as a recovery in platelet count was demonstrated during treatment. These patients first received a bolus injection followed by an infusion of 150 mg/kg or 300 mg/kg NAC per day, a higher dose compared to the case study of Shortt et al. (2013). In the study of Cabanillas and Popescu-Martinez (2015) a relapsing TTP patient went in complete remission after NAC admistration (150 mg/kg during 10 days). Proof of concept that NAC is effective as a treatment for TTP has not been demonstrated thus far, and requires preclinical animal models.

4.3   Animal models

Animal models are a valuable tool for the development and testing of new treatment strategies and for a better understanding of the pathophysiology of a disease. TTP has already been successfully induced in mice, rats and baboons. $Adamts13^{-/-}$ mice exhibit a prothrombotic and pro-inflammatory phenotype (Vanhoorelbeke and De Meyer, 2013), however a deficiency in ADAMTS13 doesn't result in the spontaneous development of TTP symptoms. Mice can develop TTP-like symptoms when using additional triggers such as the bacterial Shiga toxin or high-dose recombinant human VWF (rVWF) containing UL-VWF multimers (Schiviz et al., 2012; Motto et al., 2005). This recombinant VWF was also used to develop an acquired TTP model in rats; rats developed TTP-like symptoms when injected with a polyclonal anti-ADAMTS13 antibody, followed by an injection with rVWF (Tersteeg et al., 2015). A model for acquired TTP was generated in baboons using the monoclonal anti-ADAMTS13 antibody 3H9. This inhibitory antibody is directed against the metalloprotease domain of ADAMTS13 and inhibits ADAMTS13 activity resulting in the spontaneous development of TTP symptoms. The baboon model represents the early stage of TTP, as symptoms are not end-stage and animals recover when terminating 3H9 injections (Vanhoorelbeke and De Meyer, 2013; Feys et al. 2010b).

Chapter 5

Objectives

TTP is a life-threatening disease, if left untreated. Due to the use of plasma exchange therapy (often in combination with immunosupressive agents) for acquired TTP and plasma infusion therapy for congenital TTP, the survival rate of these patients has been raised from 10 to 80-90 percent. Nevertheless, new treatment strategies are still desirable.

Chen et al. (2011) proposed that the FDA-approved drug NAC might be a good alternative for the treatment of patients with acute TTP. NAC has a free thiol-group, which provides the ability of this drug to reduce disulphide bonds. This characteristic of NAC has already been used to treat several lung diseases by reducing the disulphide bonds linking mucin monomers, the main components of mucus. Because mucin monomers multimerize in the same way as VWF monomers, they proposed, and subsequently demostrated that NAC can also reduce VWF multimer size. Therefore, the administration of NAC could be a new treatment strategy for acute TTP.

During the first part of this project, the effect of NAC addition to human, baboon and murine ($Adamts13^{-/-}$) plasma VWF was determined in vitro. This was characterized by determining the effect of NAC on the plasma VWF- activity and multimer pattern. During the second part of this project, the effect of NAC on the prevention and treatment of acute TTP symptoms was investigated in a preclinical mouse model for congenital TTP. The use of NAC (in addition to standard plasma exchange therapy) as a treatment for acute TTP patients has already been investigated. However, due to the low number of NAC-treated patients and the inconsistent outcome, the effectiveness of NAC on the prevention and treatment of TTP is still unclear. Therefore, it needs to be investigated in preclinical animal models without plasma infusion or exchange therapy. Plasma samples of NAC-treated and control mice were tested for the presence of following TTP symptoms: thrombocytopenia, hemolytic anemia and elevated LDH activity levels. In addition, changes in human and murine VWF antigen levels and VWF multimer patterns were also analyzed.

Part II

Materials and methods

Chapter 6

In vitro effect of NAC on plasma VWF

6.1   VWF multimer analysis

To investigate the effect of NAC (Paradote, Equity Pharmaceuticals, Pretoria, South Africa) on the VWF multimer pattern in plasma, different concentrations of NAC (0 mM, 4 mM, 8 mM, 16 mM and 32 mM in 0.9% NaCl) were added to citrate-treated platelet-poor normal murine (NMP; $Adamts13^{-/-}$ mice), normal human (NHP) and baboon plasma and incubated during 30 minutes at 37 °C. The VWF multimer pattern of these samples was determined by VWF multimer analysis (6 µL for human and baboon plasma samples, 12 µL for murine plasma samples). First, the hydrophobic side of the Gelbond (Lonza, Rockland, USA) was adhered on a glass plate. Next, the casting system, composed of two glass plates (one with and one without spacer), was completed and placed in a preheated drying oven with a temperature of about 60 °C. Meanwhile, the 1.2% running gel (Table 6.1) was made. The running buffer and distilled water (dH$_2$O) were filtered (Whatmann^{TM}, 0.45 µM filter; Sigma Aldrich, St Louis, USA) before they were added to the agarose. This composition was heated and sodium dodecyl sulphate (SDS) was added. Then, the gel was added between the two glass plates. After five minutes at room temperature (RT), the gel was transferred to 4 °C for 20 minutes. In the meantime, the electrophoresis buffer (Table 6.2), sample buffer (Table 6.3) and 0.8% stacking gel (Table 6.4) were made. The stacking gel was made in the same way as the running gel. Subsequently, the hot stacking gel was added on top of the running gel and placed at RT during 30 minutes. During the multimerization of the gel, the samples were prepared. These samples were composed of 6 µL loading dye (3% bromophenol blue in ethanol), 6 µL plasma for human and baboon samples (and 54 µL sample buffer) or 12 µL plasma for murine samples (and 48 µL sample buffer). The plasma samples were directly added to the sample buffer after 30 minutes of incubation with NAC at 37 °C. Thereafter, the samples were incubated during 30 minutes at 60 °C. This ensures the inactivation of proteases. Before the gel was put on the Multiphor II (LKB Bromma, Sollentuna, Sweden), 1.5 mL of kerosene (Serva Electrophoresis GmbH, Heidelberg, Germany) was distributed on the cooling

element of the device. Kerosene ensures a better cooling and is a current conductor. Next, the buffer tanks were filled with electrophoresis buffer and Whatmann^{TM} filter papers were humidified in this buffer. These filters ensured contact between the buffer tanks and the gel. Then, 20 µL of each sample was added to the wells in the stacking gel. The voltage source was set to 160 V and a current of 15 mA ran through the gel. When the samples migrated from the wells, the voltage source was paused and the wells were filled up with stacking gel. This caused a better conduction of the current. Thereafter, the voltage source was again activated until the bromophenol blue had reached the Whatmann^{TM} paper at the side of the anode. Subsequently, the gel was rinsed in dH$_2$O for 20 minutes and dried during one hour. Then, the gel was blocked with 5% milk powder (Carl Roth GmbH + Co. KG, Karlsruhe, Germany) in tris-buffered saline (TBS, Table 6.5) with 0.05% Tween20 (Acros Organics, Geel, Belgium). After 30 minutes, the blocking solution was discarded and the gel was incubated with a polyclonal anti-human VWF antibody labelled with alkaline phosphatase (anti-VWF-AP; 1/750 in TBS) overnight. The day after, the gel was washed ten times six minutes in TBS with 0.05% Tween20. Thereafter, the gel was incubated with the colouring solution (Table 6.6) for 30 minutes to one hour. Finally, the gel was washed with dH$_2$O and dried. The percentage low molecular weight (LMW), medium molecular weight (MMW) and high molecular weight (HMW) VWF multimers was determined with densitomatric analysis using Image J (National Institutes of Health, Bethesda, Maryland). The low (band 1-5), intermediate (band 6-10), and high molecular weight (> 10 bands) multimers were selected and the density of the LMW, MMW and HMW multimers relative to the complete multimer were calculated as a percentage.

Table 6.1: Composition of 1.2% running gel.

Product	Supplier
4 mL 5x running buffer (1.875 M Tris, pH 8.8)	Sigma Aldrich, St. Louis, USA
240 mg agarose isoelectric focusing (IEF)	GE Healthcare Bio-Sciences AB, Uppsala, Sweden
100 µL 25% SDS	Acros Organics, Geel, Belgium
16 mL dH$_2$O	–

Table 6.2: Composition of electrophoresis buffer (2.5 L).

Product	Supplier
0.05 M Tris	Sigma Aldrich, St. Louis, USA
0.384 M glycine	Thermo Fisher Scientific, New Jersey, USA
0.1% SDS	Acros Organics, Geel, Belgium

Table 6.3: Composition of sample buffer (100 mL).

Product	Supplier
8 M ureum	Sigma Aldrich, St. Louis, USA
5 g SDS	Acros Organics, Geel, Belgium
10 mL 10x stock solution (10mM Tris and 1 nM EDTA, pH 8)	Sigma Aldrich, St. Louis, USA

Table 6.4: Composition of 0.8% stacking gel.

Product	Supplier
2 mL 5x stacking buffer (0.625 M Tris, pH 6.8)	Sigma Aldrich, St. Louis, USA
80 mg agarose IEF	GE Healthcare Bio-Sciences AB, Uppsala, Sweden
50 µL 25% SDS	Acros Organics, Geel, Belgium
16 mL dH$_2$O	–

Table 6.5: Composition of tris-buffered saline (TBS) buffer (1 L).

Product	Supplier
43.89 g NaCl	Carl Roth GmbH + Co. KG, Karlsruhe, Germany
12.11 g Tris	Sigma Aldrich, St. Louis, USA
HCl to adjust pH to 7.5	Acros Organics, Geel, Belgium

Table 6.6: Composition of colouring solution.

Product	Supplier
1 mL 25x AP buffer	Biorad Hercules, USA
250 µL AP reagent A	Biorad Hercules, USA
250 µL AP reagent B	Biorad Hercules, USA
24 mL dH$_2$O	–

6.2 Ristocetin/Botrocetin cofactor activity of VWF

To determine the activity levels of NMP, NHP and baboon plasma VWF, the VWF ristocetin/botrocetin cofactor assay was performed. In the absence of shear forces, human or baboon plasma VWF binds to captured recombinant GPIb fragments in the presence of ristocetin in an ELISA (enzyme-linked immunosorbent assay)-based assay (Vanhoorelbeke et al., 2000). Ristocetin is a glycoprotein antibiotic which triggers conformational changes allowing VWF to expose its GPIb binding site (Di Stasio et al., 2009). The same applies to the murine plasma VWF binding to recombinant GPIb in the presence of the snake venom botrocetin. The anti-GPIb antibody 2D4 (5 µg/mL in TBS; 100 µL/well) was coated on a microtiter plate (Greiner Bio-One

BVBA/SPRL, Wemmel, Belgium) in a wet chamber at 4°C overnight. The next day, the microtiter plate was washed three times in TBS with 0.1% Tween20 (TBS-T) and blocked during two hours at RT using TBS with 3% milk powder (200 µL/well). This blocking reduced nonspecific binding of proteins to the microtiter plate. Then, the microtiter plate was again washed three times in TBS-T and incubated with an in-house developed recombinant GPIb (rGPIb; 1 µg/mL in TBS-T; 100 µL/well) during two hours at 37 °C. Next, the microtiter plate was washed 12 times in TBS-T. For the human VWF ristocetin cofactor ELISA, 760 µg/mL ristocetin (American Biochemical & Pharmaceuticals Ltd., Epsom, UK) in TBS-T was added to the microtiter plate. For the baboon VWF ristocetin cofactor ELISA, 150 µg/mL ristocetin in TBS-T was added. For the murine VWF botrocetin cofactor activity assay, 0.1 µg/mL botrocetin (Sigma-Aldrich, Diegem, Belgium) in TBS-T was added to the microtiter plate (100 µL/well). Human, baboon and murine $Adamts13^{-/-}$ plasma samples were thawed at 37 °C during five minutes. Subsequently, these samples were incubated with 0 mM, 4 mM, 8 mM, 16 mM and 32 mM NAC (in 0.9% NaCl) for 30 minutes at 37 °C. After this incubation, the plasma samples were added directly to the microtiter plate (1/32 dilution for human and baboon plasma samples and 1/16 dilution for murine plasma samples) and these dilutions were again 1/2 serial diluted. These plasma samples were incubated during 1.5 hours at 37 °C (100 µL/well). Thereafter, the microtiter plate was washed 12 times in TBS-T and incubated with the detection antibody rabbit-anti-human VWF horseradish peroxidase (RAH-VWF-HRP; Dako, Glostrup, Denmark; 1/3000 in TBS-T; 100 µL/well) for one hour at RT. Next, the microtiter plate was washed 12 times and the colour reaction was initiated using the ELISA detection solution (160 µL/well; Table 6.7). This reaction was stopped with 4 M sulfuric acid (Acros Organics, Geel, Belgium). Finally, the absorbance at 490 nm was measured using a Fluostar Optima ELISA reader (BMG Labtech GmbH, Ortenberg, Germany). The VWF activity levels were calculated using the absorbance values of plasma samples with 0 mM NAC (Figure 6.1).

Table 6.7: Composition of the ELISA detection solution.

Product	Supplier
10 mL phosphate buffer: 0.1 M $Na_2HPO_4.2H_2O$	Acros Organics, Geel, Belgium
10 mL citrate buffer: 0.05 M citrate	Acros Organics, Geel, Belgium
8 µL H_2O_2: 35%	Acros Organics, Geel, Belgium
200 µL o-phenylenediamine (OPD): 4.6 mM	Sigma Aldrich, St. Louis, USA
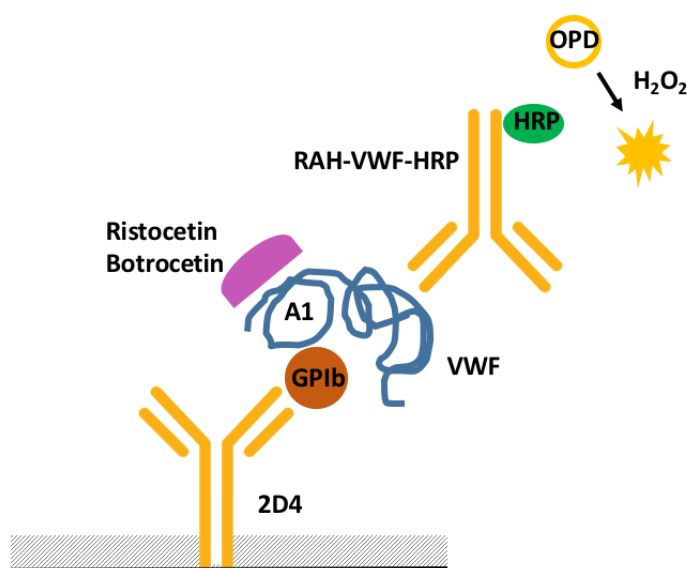
Figure 6.1: Schematic representation of the ristocetin/botrocetin cofactor activity assay. The microtiter plate was coated with the anti-GPIb antibody 2D4 that binds rGPIb. rGPIb binds the GPIb-platelet binding site in the A1 domain of VWF in the presence of ristocetin (human and baboon VWF) or botrocetin (murine VWF). VWF was subsequently detected using an HRP-coupled RAH-VWF antibody in the presence of H_2O_2 and OPD.

6.3 Platelet agglutination

To investigate the effect of NAC on the in vitro platelet agglutination, different concentrations of NAC (0 mM, 4 mM, 8 mM, 16 mM and 32 mM) in HEPES Tyrode buffer (HT buffer (Table 6.8)) were added to citrate-treated platelet-poor NHP. Before use, the 10x HT buffer had to be diluted and 5.5 mM glucose and 3.5 mg/mL bovine serum albumin (BSA) were added. Subsequently, the samples were incubated during 30 minutes at 37 °C (9/10 volume NHP, 1/10 volume NAC in HT buffer). Next, the reaction mixture (60 µL) was added to 4/5 volume of a final concentration of 200 x 10^3 lyophilized platelets/ µL (240 µL; Bio/Data Corporation, Horsham, USA). Thereafter, the agglutination was induced using 0.9 - 1.0 mg/mL ristocetin. This reaction was monitored for approximately 15 minutes by means of the aggrerometer (Chrono-Log Corporation, Havertown, USA). The agglutination percentages reached after 15 minutes for the different NAC concentrations were graphed. The experiments with the addition of 0 mM and 32 mM NAC were repeated using baboon plasma.

In addition, the breakdown of a platelet agglutinate by NAC was investigated. First, 60 µL NHP was added to 240 µL lyophilized platelets and the agglutination was induced using 0.9 - 1.0 mg/mL ristocetin. When the platelet agglutinate was formed, 0 mM or 32 mM NAC was added and the breakdown of the agglutinate was followed during approximately 30 minutes using the aggrerometer. This experiment was also repeated using baboon plasma.

Table 6.8: Composition of 10x HEPES Tyrode buffer

Product	Supplier
1.37 mM NaCl	Carl Roth GmbH + Co. KG, Karlsruhe, Germany
20 mM KCl	Acros Organics, Geel, Belgium
3 mM NaH_2PO_4	Merck KGaA, Darmstadt, Germany
10 mM $MgCl_2$	Acros Organics, Geel, Belgium
50 mM Hepes	Carl Roth GmbH + Co. KG, Karlsruhe, Germany
120 mM $NaHCO_3$	Acros Organics, Geel, Belgium
dH_2O	–

Chapter 7

Effect of NAC on TTP symptoms in mice

The effect of NAC on the prevention and treatment of TTP symptoms was studied in a congenital TTP mouse model, using $Adamts13^{-/-}$ mice (CASA/Rk-C57BL/6J-129X1/SvJ background). For this study, both female and male mice with an age between 6-9 weeks and a weight between 18-23 gram were used. All of these animal experiments were performed in accordance with protocols approved by the Institutional Animal Care and Use Committee of KU Leuven (Belgium). The injections and blood withdrawals were performed under anaesthesia via the retro-orbital plexus, using 5% isoflurane (Nicholas Piramal Limited, London, UK) in O_2.

To investigate the **prophylactic** effect of NAC on the development of acute TTP symptoms, $Adamts13^{-/-}$ mice ($n = 12$) were injected intravenously with 800 mg/kg NAC. Control mice ($n = 12$) were injected with equal volumes of saline. After 15 minutes, a dose of 2000 to 2250 U/kg rVWF (Baxalta, Vienna, Austria) was injected in all mice. This dose of rVWF triggers TTP-like symptoms in $Adamts13^{-/-}$ mice, as was described before (Schiviz et al., 2012).

To investigate the role of NAC in the **treatment** of acute TTP symptoms, $Adamts13^{-/-}$ mice ($n = 10$) were first injected with 2000 to 2250 U/kg rVWF. After 1 and 12 hours, mice were injected with a dose of 800 mg/kg NAC. Control mice ($n = 10$) were injected with equal volumes of saline. (Figure 7.1)

Blood samples were collected by retro-orbital puncture at baseline (day -7) and 24 hours after rVWF injections on 3.8% trisodium citrate (Acros Organics, Geel, Belgium; 1 volume to 7 volumes of blood) or 0.5 M ethylenediaminetetraacetic acid (EDTA; Acros Organics, Geel, Belgium; 1 volume to 15 volumes of blood). Plasma was obtained from the citrated blood after centrifugation during 6 minutes at 2500 g and was afterwards stored at -80 °C. EDTA-treated blood samples were used for total blood cell counts using a hematocounter device (Hemavet 950; Drew Scientific, Dallas, USA) .
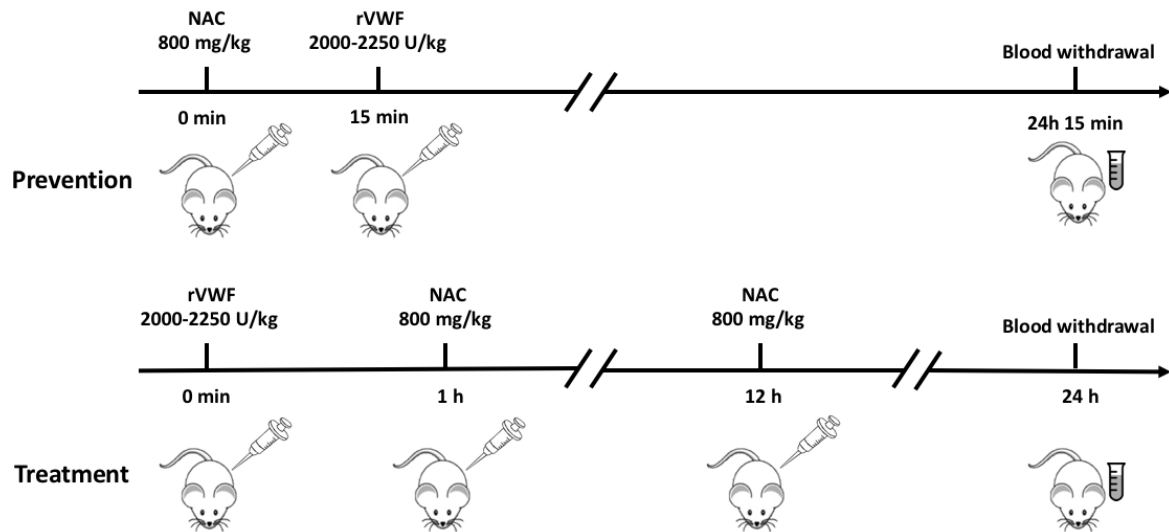
Figure 7.1: Timeline injections and blood withdrawals in *Adamts13* deficient mice of the prevention and treatment group. *Adamts13*$^{-/-}$ mice from the prevention group were first injected with 800 mg/kg NAC and thereafter with 2000 to 2250 U/kg rVWF. *Adamts13*$^{-/-}$ mice from the treatment group were first injected with 2000 to 2250 U/kg rVWF and thereafter with 800 mg/kg NAC. Blood was taken 24 hours after rVWF injections. Control mice were injected with saline instead of NAC.

7.1 muVWF antigen levels

The murine VWF (muVWF) antigen levels in the citrate-treated plasma samples were determined using a sandwich ELISA. The polyclonal antibody rabbit-anti-human VWF (RAH-VWF; Dako, Glostrup, Denmark; 1/1000 in phosphate buffered saline (PBS, Table 7.1); 100 µL/well) was coated on a microtiter plate in a wet chamber at 4 °C overnight. The next day, the microtiter plate was washed three times in PBS with 0.1% Tween20 (PBS-T) and blocked during two hours at RT using PBS with 3% milk powder (200 µL/well). Afterwards, the microtiter plate was washed three times in PBS-T. The plasma samples were thawed at 37 °C during five minutes and a 1/10 dilution of these samples was made in PBS with 0.3% milk powder. From these dilutions, 1/2 serial dilutions were made and then incubated during one hour at 37 °C (100 µL/well). As positive control sample and calibrator, NMP from *Adamts13*$^{-/-}$ mice was used. Thereafter, the microtiter plate was washed six times in PBS-T and incubated with the biotinylated anti-VWF antibodies 2C12bio and 15H2bio (1 µg/mL in PBS with 0.3% milk powder; 100 µL/well) during one hour at RT. Next, the microtiter plate was washed six times in PBS-T and incubated with streptavidin-HRP

(Roche Diagnostics GmbH, Mannheim, Germany; 1/10.000 in PBS + 0.3% milk powder; 100 µL/well) during one hour at RT. Then, the microtiter plate was washed eight times and the colour reaction was initiated and stopped as described before. Finally, the absorbance at 490 nm was measured using a Fluostar Optima ELISA reader. The muVWF antigen levels were calculated using the absorbance values of the calibrator NMP (Figure 7.2).

Table 7.1: Composition of phosphate buffered saline (PBS) buffer (1 L).

Product	Supplier
8.0 g NaCl	Carl Roth GmbH + Co. KG, Karlsruhe, Germany
0.2 g KCl	Acros Organics, Geel, Belgium
1.15 g $Na_2HPO_4.2H_2O$	Acros Organics, Geel, Belgium
0.2 g KH_2PO_4	Acros Organics, Geel, Belgium
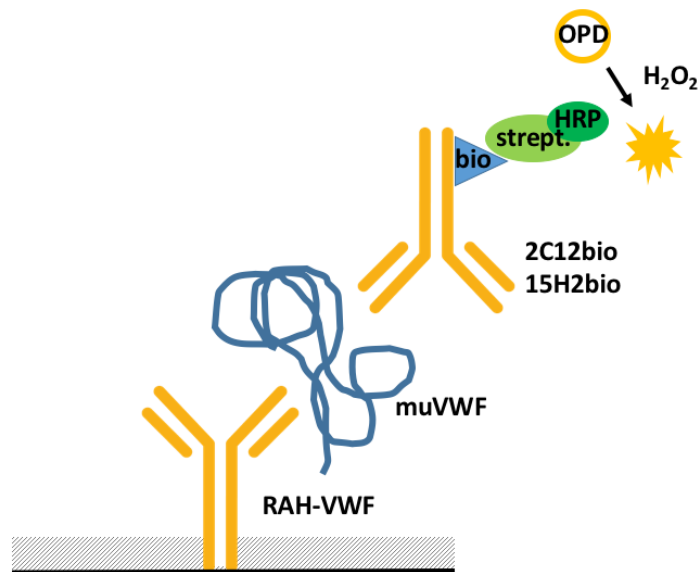
Figure 7.2: Schematic representation of the muVWF antigen ELISA. The microtiter plate was coated with a RAH-VWF antibody that catches VWF from murine plasma. Murine VWF was subsequently detected using two biotinylated muVWF antibodies and HRP-coupled streptavidin in the presence of H_2O_2 and OPD.

7.2 huVWF antigen levels

Because the *Adamts13$^{-/-}$* mice were injected with recombinant human VWF (huVWF), the huVWF antigen levels in the murine plasma samples were also determined using a sandwich ELISA. The monoclonal anti-huVWF antibody 6D1 (5 µg/ml in PBS;

100 µL/well) was coated on a microtiter plate in a wet chamber at 4 °C overnight. The next day, the microtiter plate was washed three times in PBS-T and blocked during two hours at RT using PBS with 3% milk powder (200 µL/well). Afterwards, the microtiter plate was washed three times in PBS-T. The plasma samples were thawed at 37 °C during 5 minutes and a 1/100 dilution of the plasma samples was made in PBS with 0.3% milk powder. As positive control sample and calibrator, a 1/80 dilution of NHP was made. These dilutions were subjected to 1/2 serial dilutions and subsequently incubated during 1.5 hours at 37 °C (100 µL/well). Thereafter, the microtiter plate was washed six times in PBS-T and incubated with the detection antibody RAH-VWF-HRP (1/3000 in PBS with 0.3% milk powder; 100 µL/well) during one hour at 37 °C. Next, the microtiter plate was washed six times and the colour reaction was initiated and stopped as described before. Finally, the absorbance at 490 nm was measured using the Fluostar Optima ELISA reader. The huVWF antigen levels were calculated using the absorbance values of the calibrator NHP (Figure 7.3).
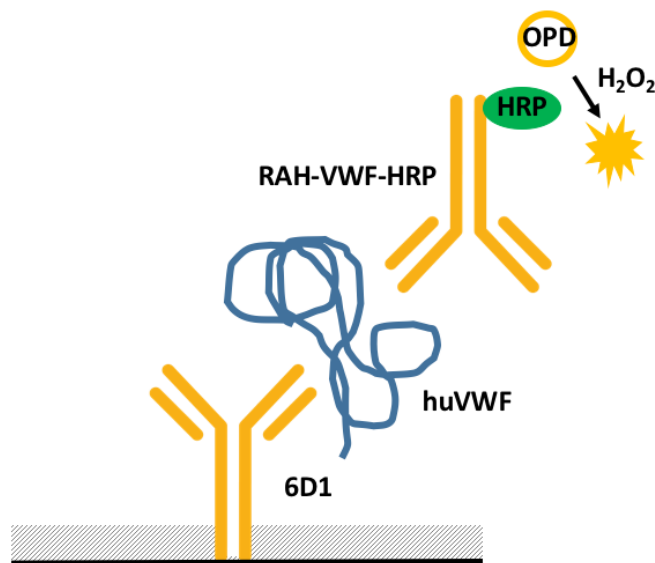
Figure 7.3: Schematic representation of the huVWF antigen ELISA. The microtiter plate was coated with the anti-VWF antibody 6D1 that catches human VWF from murine plasma. Human VWF was subsequently detected using the HRP-coupled RAH-VWF antibody in the presence of H_2O_2 and OPD.

7.3 LDH activity levels

Lactate dehydrogenase (LDH) is an oxidoreductase that catalyses the interconversion of pyruvate and lactate, with the concomitant interconversion of NADH and NAD^+.

This enzyme is released in the bloodstream in case of tissue damage, which occurs in TTP. LDH is a stable enzyme and therefore its activity can be used to quantify tissue damage. This activity is measured using an LDH activity colorimetric assay kit (Biovision, Milpitas, USA). In this assay, LDH catalyses the conversion of NAD^+ to NADH. The produced NADH subsequently interacts with a probe which results in a colour reaction. To determine the LDH activity levels in murine plasma, 1 µL of the murine plasma sample was added to 49 µL of Assay Buffer in a microtiter plate. As a calibrator, several dilutions of the NADH Standard (0 mM, 2.5 mM, 5.0 mM, 7.5 mM, 10.0 mM, 12.5 mM) in Assay Buffer with a final volume of 50 µL were also added to the microtiter plate. Next, 50 µL of the Reaction Mix (1/25 Substrate Mix Solution in Assay Buffer) was added to each well. Finally, the absorbance at 450 nm was measured using the Fluostar Optima ELISA reader. This absorbance value was measured every minute during 30 minutes. The LDH activity levels were eventually determined using the absorbance values of the calibrator.

7.4 VWF multimer analysis

The effect of NAC administration on the VWF multimer pattern in murine plasma samples obtained 6 (1 µL plasma) and 24 (6 µL plasma) hours after rVWF administration was analyzed as described before. The low, intermediate, and high molecular weight multimers were selected and the density of the LMW, MMW and HMW multimers relative to the complete multimer were calculated as a percentage.

7.5 Statistical analysis

All data are presented as mean ± standard deviation. Statistical comparison between two (in)dependent groups were performed by a two-tailed (un)paired Student's *t*-test. Statistical comparison between different (> 2) independent groups were performed by a one-way ANOVA analysis with multiple comparisons and Bonferroni correction. These statistical analyzes were done using GraphPad Prism 6 (GraphPad Software Inc., La Jolla, USA).

Part III

Results and Discussion

Chapter 8

In vitro effect of NAC on plasma VWF

8.1 VWF multimer analysis

The ability of NAC to reduce VWF multimer size, analogous to its effect on mucins, was determined. The VWF multimer pattern of plasma, to which different concentrations of NAC were added, was analysed using a multimer agarose gel (1.2% running gel and 0.8% stacking gel). Three different NHP, baboon and NMP ($Adamts13^{-/-}$ mice) plasma samples were pre-incubated with 0 mM, 4 mM, 8 mM, 16 mM or 32 mM NAC. The percentage LMW, MMW and HMW VWF multimers was determined for each of these samples (Table 8.1). The reduction of HMW VWF multimers in NHP was significant (P<0.001) for the addition of 4 mM NAC and higher concentrations (Figure 8.1). The reduction of HMW VWF multimers in baboon plasma was significant (P<0.001) for the addition of 8 mM NAC and higher concentrations (Figure 8.2). The reduction of HMW VWF multimers in NMP was only significant (P<0.001) for the addition of 16 mM NAC. No VWF multimers were observed when 32 mM NAC was added to NMP. This can be explained by the low molecular weight of the residual multimers, which was probably under the detection limit of the VWF multimer analysis method (Figure 8.3).

These results demonstrate that NAC is able to efficiently reduce HMW VWF multimers in plasma from humans, baboons and mice in a concentration-dependent way.

Table 8.1: HMW VWF multimer percentage of NHP, baboon and NMP plasma VWF, pre-incubated with different concentrations of NAC.

	0 mM NAC	4 mM NAC	8 mM NAC	16 mM NAC	32 mM NAC
human plasma	32.28 ± 1.48 %	14.68 ± 3.42 %	6.87 ± 2.71 %	0.00 ± 0.00 %	0.00 ± 0.00 %
baboon plasma	34.40 ± 3.18 %	36.24 ± 2.12 %	18.55 ± 1.43 %	0.00 ± 0.00 %	0.00 ± 0.00 %
murine plasma	42.45 ± 2.64 %	39.66 ± 1.30 %	38.39 ± 2.34 %	8.22 ± 4.63 %	*below detection limit*
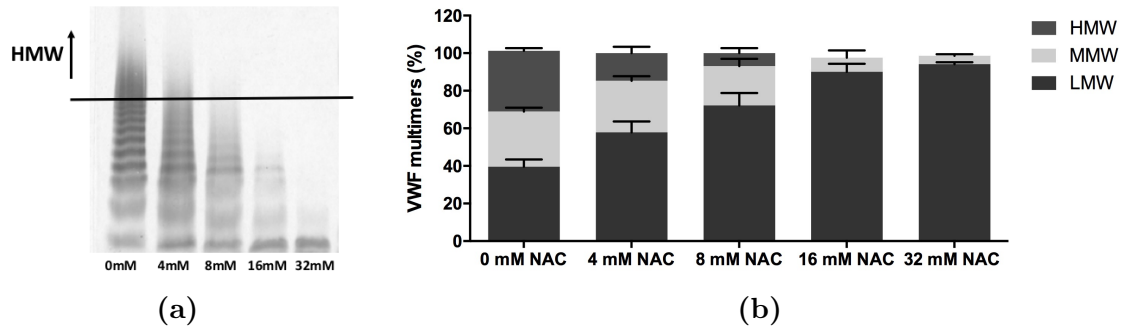
Figure 8.1: VWF multimer pattern of NHP, pre-incubated with different concentrations of NAC. (a) A representative image of the multimer pattern after incubation with NAC. (b) VWF multimer analysis was performed and the percentages HMW, MMW and LMW multimers were calculated using densitometry analysis ($n = 3$).
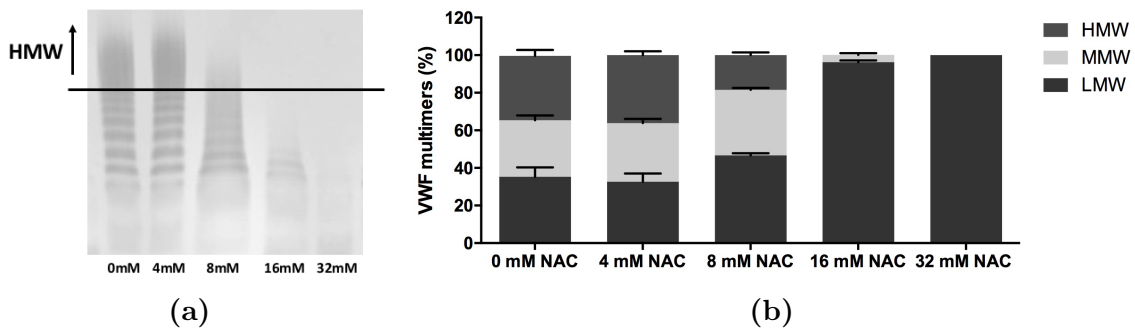
Figure 8.2: VWF multimer pattern of baboon plasma, pre-incubated with different concentrations of NAC. (a) A representative image of the multimer pattern after incubation with NAC. (b) VWF multimer analysis was performed and the percentages HMW, MMW and LMW multimers were calculated using densitometry analysis ($n = 3$).
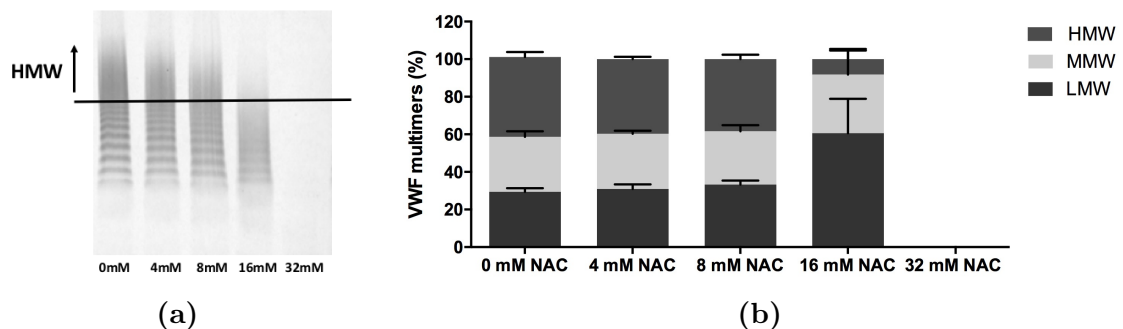
Figure 8.3: VWF multimer pattern of NMP, pre-incubated with different concentrations of NAC. (a) A representative image of the multimer pattern after incubation with NAC. (b) VWF multimer analysis was performed and the percentages HMW, MMW and LMW multimers were calculated using densitometry analysis. The multimer pattern after pre-incubation with 32 mM NAC could not be analysed and is probably under the detection limit of the VWF multimer analysis method ($n = 3$).

8.2 Ristocetin/botrocetin cofactor activity of VWF

In circulation, the platelet GPIb binding site within the VWF A1 domain is only exposed in the elongated form of VWF (Crawley et al., 2011). The in vitro interaction between platelet GPIb and VWF is promoted by ristocetin or botrocetin and is dependent on the presence of HMW VWF multimers (Fischer et al., 1996; Federici et al., 1989). In addition, Chen et al. (2011) showed that NAC is able to disrupt the intrachain disulphide bond of the VWF A1 domain which inhibits the platelet GPIb binding.

Therefore, the ability of NAC to reduce the ristocetin/botrocetin cofactor activity of VWF in plasma from humans (ristocetin), baboons (ristocetin) and mice (botrocetin) was determined (Table 8.2). Three different NHP (Figure 8.4), baboon (Figure 8.5) and NMP (*Adamts13$^{-/-}$* mice, Figure 8.6) plasma samples were pre-incubated with 0 mM, 4 mM, 8 mM, 16 mM or 32 mM NAC. The VWF activity levels of plasma with 0 mM NAC were set to 100 %. The activity of VWF in NHP and baboon plasma reduced each time significantly (P<0.001) when adding a higher concentration of NAC. The VWF activity in NMP was only significantly (P<0.001) reduced when adding 32 mM NAC.

These results demonstrate that NAC is able to efficiently reduce the ristocetin/ botrocetin cofactor activity of VWF in plasma from humans, baboons and mice in a concentration-dependent way.

Table 8.2: Ristocetin/botrocetin cofactor activity of NHP, baboon and NMP plasma VWF, pre-incubated with different concentrations of NAC.

	4 mM NAC	8 mM NAC	16 mM NAC	32 mM NAC
human plasma	76.55 ± 1.92 %	41.17 ± 1.43 %	21.18 ± 2.40 %	12.69 ± 0.87 %
baboon plasma	82.77 ± 5.56 %	12.26 ± 3.86 %	*below detection limit*	*below detection limit*
murine plasma	93.50 ± 14.44 %	94.63 ± 16.27 %	80.64 ± 4.08 %	19.86 ± 4.96 %
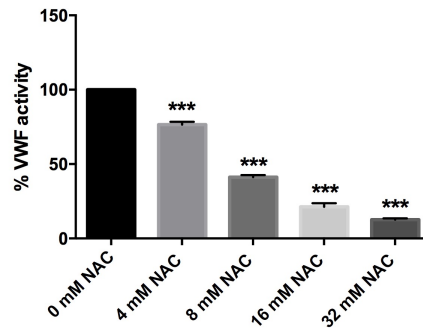
Figure 8.4: VWF ristocetin cofactor activity of NHP, pre-incubated with different concentrations of NAC. In NHP samples, VWF ristocetin cofactor activity levels were determined using an ELISA-based assay and compared to the VWF activity levels of NHP + 0 mM NAC ($n = 3$). Significance levels are indicated by asterixes (*<0.05, **<0.01, ***<0.001).
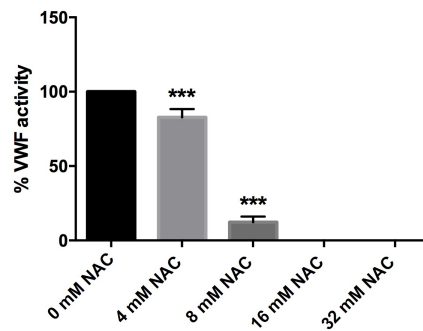
Figure 8.5: VWF ristocetin cofactor activity of baboon plasma, pre-incubated with different concentrations of NAC. In baboon plasma samples, VWF ristocetin cofactor activity levels were determined using an ELISA-based assay and compared to the VWF activity levels of baboon plasma + 0 mM NAC. The VWF activity after pre-incubation with 16 and 32 mM NAC was under the detection limit of the ristocetin cofactor assay ($n = 3$). Significance levels are indicated by asterixes (*<0.05, **<0.01, ***<0.001).
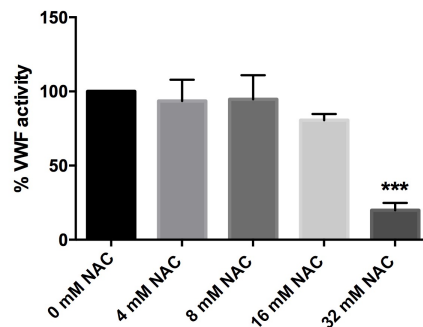
Figure 8.6: VWF botrocetin cofactor activity of NMP, pre-incubated with different concentrations of NAC. In NMP samples, VWF botrocetin cofactor activity levels were determined using an ELISA-based assay and compared to the VWF activity levels of NMP + 0 mM NAC ($n = 3$). Significance levels are indicated by asterixes (*<0.05, **<0.01, ***<0.001).

8.3   Platelet agglutinate formation

The ability of NAC to reduce the formation of VWF-containing platelet agglutinates in vitro was also investigated. As in the ristocetin cofactor assay, platelet agglutination requires a ristocetin-mediated binding of VWF to platelet GPIb and is most functional in the presence of HMW VWF multimers.

The agglutination of NHP, pre-incubated with different concentrations of NAC, was induced with ristocetin and subsequently monitored using the aggregometer. Three different NHP samples, pre-incubated with 0 mM, 4 mM, 8 mM, 16 mM or 32 mM NAC, were analysed. The average final (after 12 minutes) agglutination percentage for the different NAC concentrations was determined and compared. The final agglutination percentages of NHP pre-incubated with 16 mM and 32 mM NAC were significantly ($P<0.05$) lower compared to NHP pre-incubated with 0 mM NAC (Figure 8.7).

The formation of a platelet agglutinate was repeated with three baboon plasma samples, pre-incubated with 0 mM or 32 mM NAC. This experiment had similar results compared to NHP: platelet agglutination was impaired in the presence of 32 mM NAC (Figure 8.8).

These results demonstrate that NAC is able to efficiently reduce VWF-dependent platelet agglutination with plasma from humans and baboons in a concentration-dependent manner.

(a)

(b)
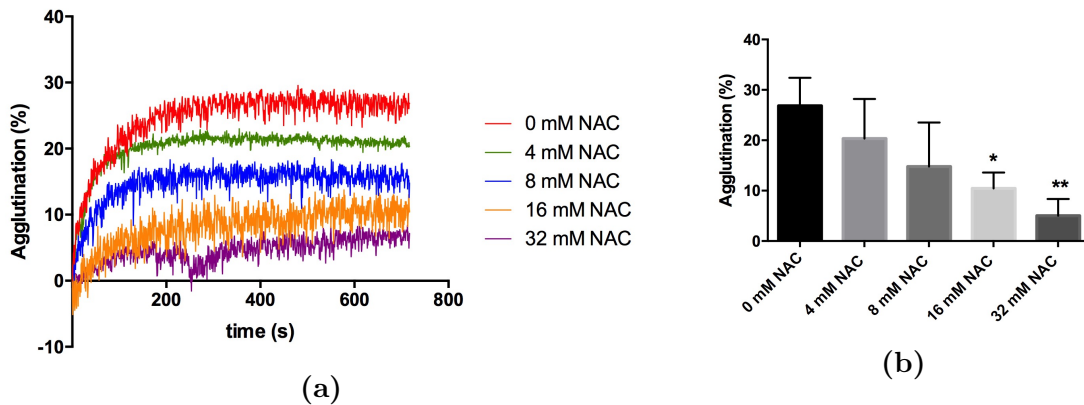
Figure 8.7: The formation of a platelet agglutinate using NHP, pre-incubated with different concentrations of NAC (a) The agglutination percentage was measured for NHP pre-incubated with 0 mM, 4 mM, 8mM, 16 mM and 32 mM NAC. Representative traces are shown. (b) The percentage of agglutination after 12 minutes for the five different concentrations of NHP with NAC was calculated ($n = 3$). Significance levels are indicated by asterixes (*<0.05, **<0.01, ***<0.001).
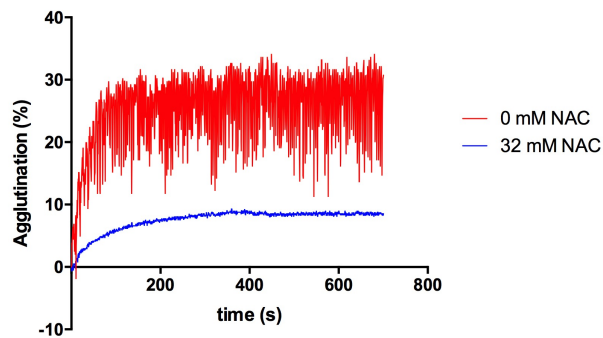
Figure 8.8: The formation of a platelet agglutinate using baboon plasma, pre-incubated with different concentrations of NAC. The agglutination percentage was measured for baboon plasma pre-incubated with 0 mM and 32 mM NAC. Representative traces are shown.

Chapter 9

Effect of NAC on TTP symptoms in mice

9.1 Prophylactic treatment of TTP in mice with NAC

The ability of NAC to reduce VWF- multimer size and activity in plasma from *Adamts13*$^{-/-}$ mice was demonstrated. Therefore, a congenital TTP mouse model was used to investigate the prophylactic effect of NAC on the development of TTP symptoms. In this model, *Adamts13*$^{-/-}$ mice were triggered with 2000 to 2250 U/kg rVWF, depending on the sensitivity of the rVWF batch, to induce TTP-like symptoms such as thrombocytopenia, hemolytic anemia and organ damage (Schiviz et al., 2012). Mice ($n = 12$) were injected with 800 mg/kg NAC, 15 minutes before rVWF injection. As a control, mice ($n = 12$) were injected with saline before rVWF injection.

9.1.1 Blood/plasma measurements

EDTA anticoagulated blood samples of control mice and mice that received prophylactic NAC were investigated for the presence of thrombocytopenia and hemolytic anemia.

At baseline, control mice demonstrated a mean platelet count of $642 \pm 61 \times 10^3$ platelets/µL, and mice that received prophylactic NAC had an average platelet count of $644 \pm 78 \times 10^3$ platelets/µL. For both groups, there was a significant (P<0.05) decrease in platelet counts, 24 hours after rVWF injection. However, mice that received prophylactic NAC had a significantly (P<0.001) higher average platelet count compared to the control group (control: $251 \pm 137 \times 10^3$ platelets/µL; NAC: $492 \pm 181 \times 10^3$ platelets/µL) (Figure 9.1).

In addition, hemoglobin (Hb) levels, which are low in the case of hemolytic anemia, were determined. At baseline, control mice demonstrated a mean Hb level of 10.5 ± 0.5 g/dL and mice that received prophylactic NAC had an average Hb level of 9.9 ± 0.6 g/dL. For both groups, there was a significant (P<0.05) decrease in Hb levels,

after 24 hours. However, mice that received prophylactic NAC had a significantly ($P<0.001$) higher average Hb level compared to the control group (control: 8.5 ± 0.5 g/dL; NAC: 9.4 ± 0.4 g/dL) (Figure 9.2).
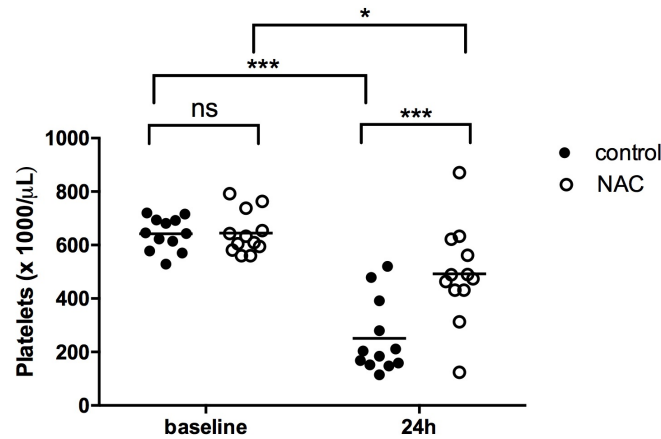
Figure 9.1: Prophylactic administration of NAC is effective in preventing thrombocytopenia in mice. 800 mg/kg NAC (or saline in controls) was administered 15 minutes before injection of rVWF. A total blood cell count was performed on EDTA anticoagulated blood at baseline and 24 hours after rVWF injection. Significance levels are indicated by asterixes (*<0.05, **<0.01, ***<0.001).
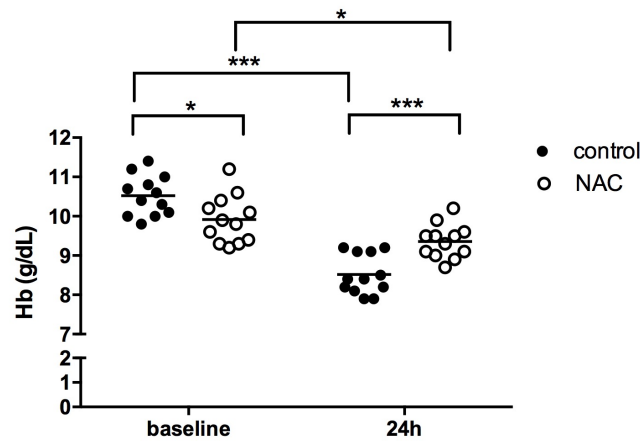
Figure 9.2: Prophylactic administration of NAC is effective in preventing hemolytic anemia in mice. 800 mg/kg NAC (or saline in controls) was administered 15 minutes before injection of rVWF. A total blood cell count was performed on EDTA anticoagulated blood at baseline and 24 hours after rVWF injection. Significance levels are indicated by asterixes (*<0.05, **<0.01, ***<0.001).

Additionally, LDH activity levels were determined in citrated plasma samples to measure tissue damage. At baseline, control mice demonstrated a mean LDH activity level of 4.12 ± 7.73 U/L and mice that received prophylactic NAC had an average LDH activity of 16.55 ± 27.09 U/L. For both groups, there was a significant (P<0.05) increase in LDH activity, 24 hours after rVWF injection. However, mice that received prophylactic NAC had a significantly (P< 0.001) lower average LDH activity level compared to the control group (control: 645.43 ± 174.93 U/L; NAC: 174.48 ± 212.91 U/L) (Figure 9.3).
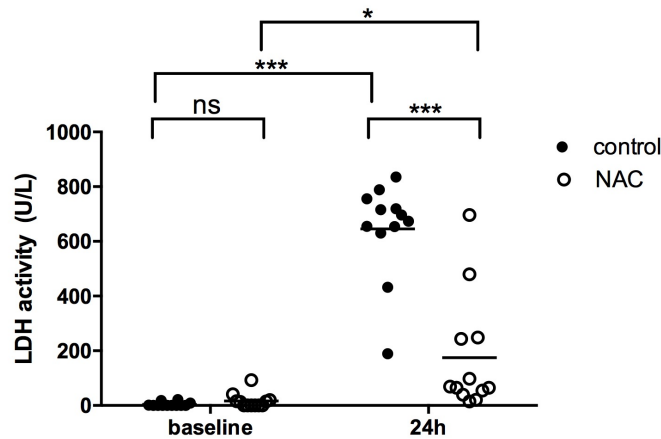
Figure 9.3: Prophylactic administration of NAC is effective in preventing tissue damage in mice. 800 mg/kg NAC (or saline in controls) was administered 15 minutes before injection of rVWF. LDH activity levels in citrated plasma samples were determined at baseline and 24 hours after rVWF injection using an LDH colorimetric assay kit. Significance levels are indicated by asterixes (*<0.05, **<0.01, ***<0.001).

These results demonstrate that the prophylactic administration of NAC is effective in preventing the onset of acute TTP symptoms, including thrombocytopenia, hemolytic anemia and tissue damage, in a congenital mouse model for TTP.

9.1.2 VWF antigen levels

Endogenous VWF levels can increase due to endothelial cell activation caused by tissue damage (de Wit et al., 2003) and the clearance of VWF is suggested to be dependent on its multimeric size (Pruss et al., 2012; Shida et al., 2013). Therefore, it was determined if the prophylactic administration of NAC is able to reduce murine VWF- and recombinant human VWF antigen levels. The muVWF- and rVWF antigen levels in citrated plasma samples were determined using a muVWF- and huVWF antigen ELISA and are expressed as a percentage of NMP ($Adamts13^{-/-}$) or NHP

VWF antigen levels. The muVWF levels of NMP and huVWF levels of NHP were set to 100%. At baseline, control mice demonstrated a mean muVWF antigen level of 112 ± 18 % and mice that received prophylactic NAC had 115 ± 25 % muVWF. For both groups, there was a significant (P<0.01) increase in muVWF antigen levels, 24 hours after rVWF injection. However, mice that received prophylactic NAC had significantly (P<0.01) lower muVWF antigen levels compared to control mice (control: 250 ± 96 %; NAC: 159 ± 29 %) (Figure 9.4). The rVWF antigen levels were also significantly (P<0.05) higher in control mice (204 ± 214 %) compared to mice that received prophylactic NAC (51 ± 34 %) (Figure 9.5).

These results demonstrate that the prophylactic administration of NAC is able to efficiently reduce and/or prevent the increase of murine VWF antigen levels and to reduce recombinant human VWF antigen levels in a congenital mouse model for TTP.
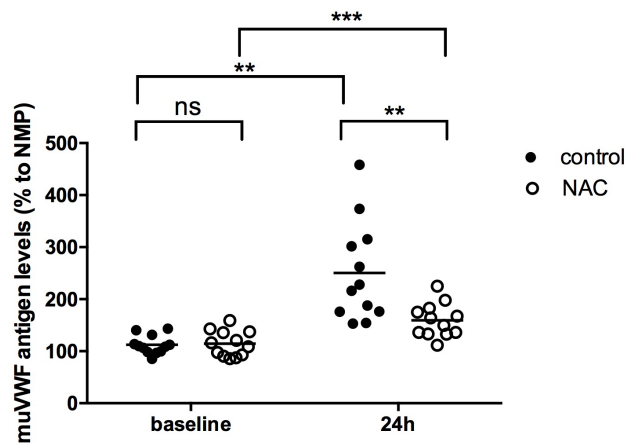
Figure 9.4: Prophylactic administration of NAC is effective in reducing mu-VWF levels in mice. 800 mg/kg NAC (or saline in controls) was administered 15 minutes before injection of rVWF. muVWF antigen levels in citrated plasma samples were determined at baseline and 24 hours after rVWF injection using ELISA and compared to the percentage of VWF in NMP. Significance levels are indicated by asterixes (*<0.05, **<0.01, ***<0.001).
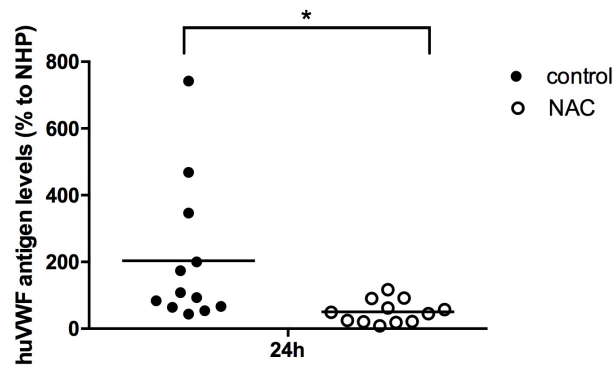
Figure 9.5: Prophylactic administration of NAC is effective in reducing recombinant huVWF levels in mice. 800 mg/kg NAC (or saline in controls) was administered 15 minutes before injection of rVWF. rVWF antigen levels in citrated plasma samples were determined at baseline and 24 hours after rVWF injection using ELISA and compared to the percentage of VWF in NHP. Significance levels are indicated by asterixes (*<0.05, **<0.01, ***<0.001).

9.1.3 VWF multimer pattern

The ability of NAC to reduce VWF multimer size in vitro in murine plasma was already demonstrated. Therefore, it was investigated if NAC is also able to exhibit this feature in the mice that received prophylactic NAC.

Twenty-four hours after rVWF injection, the VWF multimer patterns of citrated plasma from control mice and mice that received prophylactic NAC were compared (control: $n = 12$; NAC: $n = 12$). The percentage HMW VWF multimers of both groups did not differ significantly (control: 23.7 ± 2.3 %; NAC: 23.8 ± 5.1 %) (Figure 9.6, Figure 9.7).

The half-life of NAC in humans is only about 6 hours (Knudsen et al., 2004) and NAC has been shown to have an effect on VWF multimer size, 4 and 8 hours after administration (Chen et al., 2011). Therefore, the experiment was repeated using plasma samples that were obtained 6 hours after rVWF injection (control: $n = 3$; NAC: $n = 3$). The percentage HMW VWF multimers of all mice that received prophylactic NAC (24.7 ± 2.4 %) was lower compared to the HMW VWF multimer percentage of control mice (36.5 ± 0.6 %) (Figure 9.8, Figure 9.9). Because of the low number of test subjects, these results should be interpreted more as indicative rather than statistically significant.

Six hours after rVWF injection, the prophylactic administration of NAC is able to reduce disulphide bonds in circulating VWF multimers in a congenital mouse model for TTP. However, this effect can no longer be observed when plasma samples are obtained 24 hours after rVWF injection.
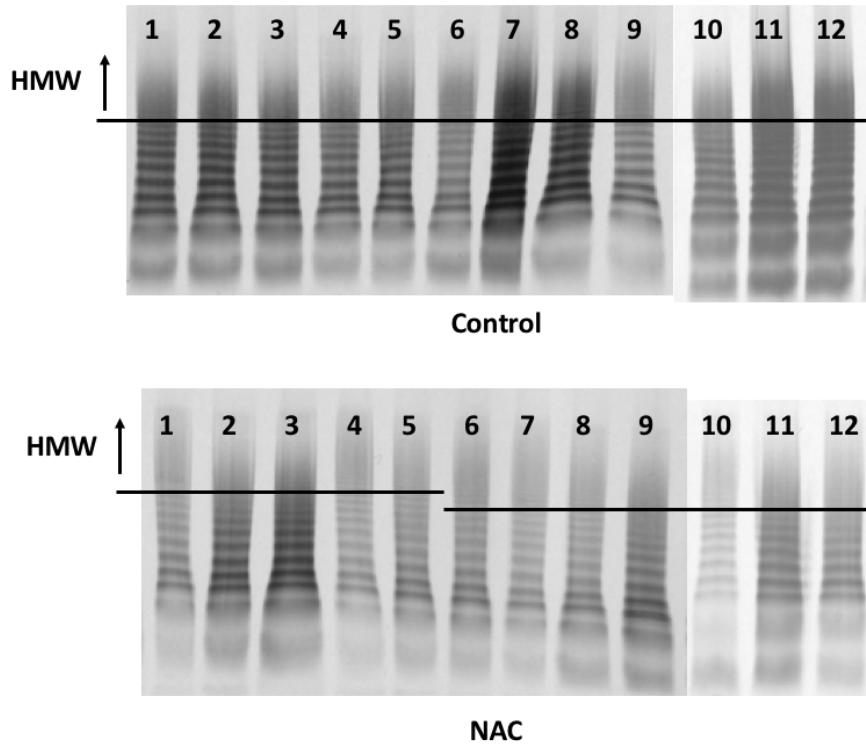
Figure 9.6: VWF multimer size of mice receiving prophylactic NAC is not reduced, 24 hours after rVWF injection. 800 mg/kg NAC (or saline in controls) was administred 15 minutes before injection of rVWF. 6 µL citrated plasma, obtained 24 hours after rVWF injection, was loaded on a 1.2% multimer agarose gel. An image of the multimer agarose gels is displayed for control mice ($n = 12$, top) and mice that received prophylactic NAC ($n = 12$, bottom) .
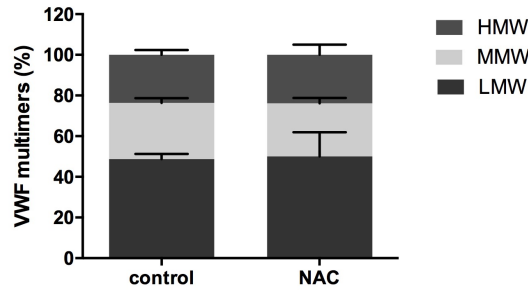
Figure 9.7: The percentage of HMW, MMW and LMW VWF multimers of mice with prophylactic NAC administration, 24 hours after rVWF injection. VWF multimer analysis was performed and the percentages HMW, MMW and LMW multimers were calculated using densitometry analysis ($n = 12$).
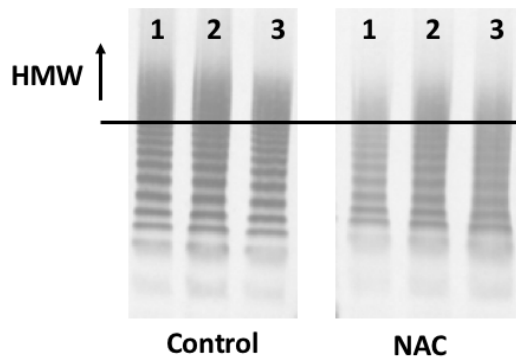
Figure 9.8: VWF multimer size of mice receiving prophylactic NAC is reduced, 6 hours after rVWF injection. 800 mg/kg NAC (or saline in controls) was administred 15 minutes before injection of rVWF. 1 µL citrated plasma, obtained 6 hours after rVWF injection, was loaded on a 1.2% multimer agarose gel. An image of the multimer agarose gels is displayed for control mice ($n = 3$, left) and mice that received prophylactic NAC ($n = 3$, right).
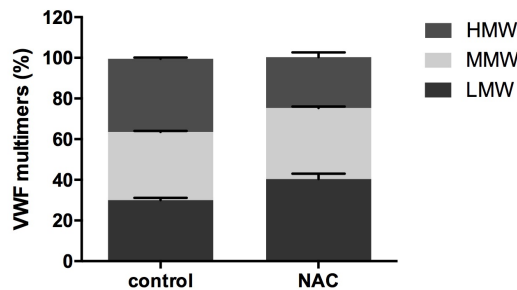
Figure 9.9: The percentage of HMW, MMW and LMW VWF multimers of mice with prophylactic NAC administration, 6 hours after rVWF injection. VWF multimer analysis was performed and the percentages HMW, MMW and LMW multimers were calculated using densitometry analysis ($n = 3$).

In conclusion, the prophylactic administration of a single dose of 800 mg/kg NAC is effective in reducing circulating VWF- multimers and antigen levels. Accordingly, NAC can efficiently prevent the development of acute TTP symptoms, including thrombocytopenia, hemolytic anemia and tissue damage, in a congenital mouse model for TTP.

9.2 Treatment of TTP in mice with NAC

The congenital TTP mouse model was also used to investigate the effect of NAC on the treatment of acute TTP. This is more clinically relevant as new treatment strategies are needed to resolve already existing acute TTP symptoms in patients. *Adamts13*$^{-/-}$ mice were triggered with 2000 to 2250 U/kg rVWF, depending on the sensitivity of the rVWF batch, to induce TTP-like symptoms. Next, the mice ($n = 10$) were injected with 800 mg/kg NAC, 1 and 12 hours after rVWF injection. In addition, control mice ($n = 10$) were injected with saline instead of NAC.

9.2.1 Blood/plasma measurements

EDTA anticoagulated blood samples of control mice and NAC-treated mice were analysed for the presence of thrombocytopenia and hemolytic anemia.

At baseline, control mice demonstrated a mean platelet count of $626 \pm 77 \times 10^3$ platelets/µL, and NAC-treated mice had an average platelet count of $621 \pm 74 \times 10^3$ platelets/µL. For both groups, platelet counts had significantly (P<0.001) decreased, 24 hours after rVWF injection (control: $267 \pm 123 \times 10^3$ platelets/µL; NAC: $245 \pm 149 \times 10^3$ platelets/µL), indicating thrombocytopenia in both groups. (Figure 9.10).

In addition, Hb levels were determined. At baseline, control mice demonstrated a mean Hb level of 11.0 ± 1.1 g/dL and NAC-treated mice had an average Hb level of 10.9 ± 1.3 g/dL. Twenty-four hours after rVWF injection, control mice had significantly (P< 0.001) decreased Hb levels (8.2 ± 0.6 g/dL), indicating hemolytic anemia. NAC-treated mice had significantly (P<0.01) higher levels of Hb (9.5 ± 1.1 g/dL) compared to the control group, 24 hours after rVWF injection, but still significantly (P<0.01) lower Hb levels than at baseline (Figure 9.11).
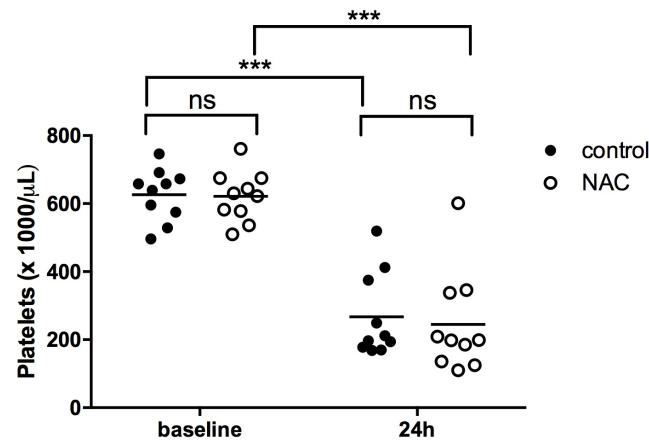
Figure 9.10: Treatment with NAC is not effective in improving thrombocytopenia in mice. 800 mg/kg NAC (or saline in controls) was administered one and 12 hours after injection of rVWF. A total blood cell count was performed on EDTA anticoagulated blood at baseline and 24 hours after rVWF injection. Significance levels are indicated by asterixes (*<0.05, **<0.01, ***<0.001).
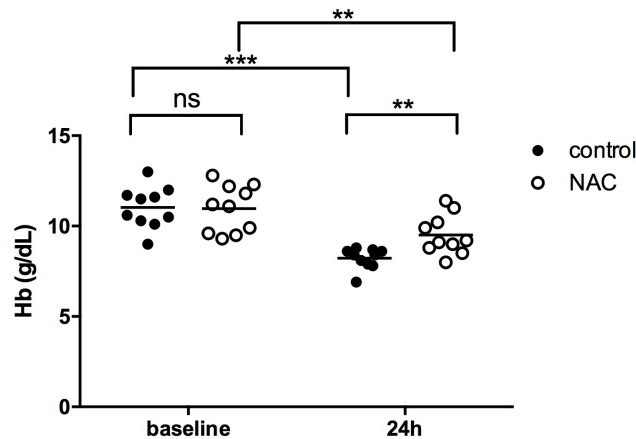
Figure 9.11: Treatment with NAC is able to improve hemolytic anemia in mice. 800 mg/kg NAC (or saline in controls) was administered one and 12 hours after injection of rVWF. A total blood cell count was performed on EDTA anticoagulated blood at baseline and 24 hours after rVWF injection. Significance levels are indicated by asterixes (*<0.05, **<0.01, ***<0.001).

Additionally, LDH activity levels were determined in citrated plasma samples to measure tissue damage. At baseline, control mice demonstrated a mean LDH activity level of 8.99 ± 17.24 U/L and NAC-treated mice had an LDH activity of 9.49 ± 16.04 U/L. Twenty-four hours after rVWF injection, LDH activity levels had increased significantly ($P<0.001$), both in control- as NAC-treated mice, with levels of 758.34 ± 313.56 and 542.92 ± 339.57 U/L respectively (Figure 9.12).
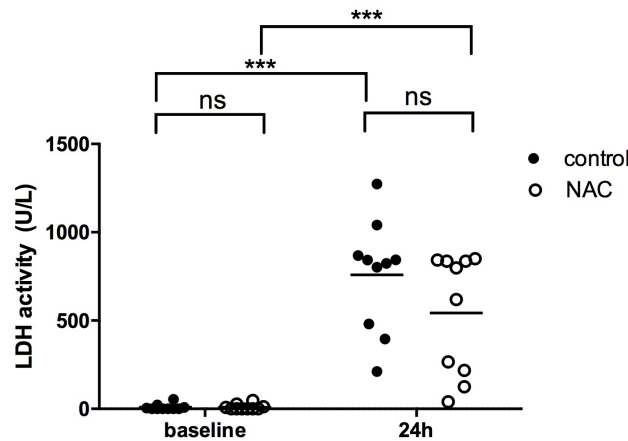
Figure 9.12: Treatment with NAC is not effective in improving tissue damage in mice. 800 mg/kg NAC (or saline in controls) was administered one and 12 hours after injection of rVWF. LDH activity levels in citrated plasma samples were determined at baseline and 24 hours after rVWF injection using an LDH colorimetric assay kit. Significance levels are indicated by asterixes (*<0.05, **<0.01, ***<0.001).

These results demonstrate that NAC is not effective in resolving already existing TTP symptoms, including thrombocytopenia and tissue damage, in a congenital TTP mouse model.

9.2.2 VWF antigen levels

The ability of NAC to reduce murine- and recombinant human VWF antigen levels in mice with acute TTP symptoms was also investigated. The muVWF- and rVWF antigen levels in citrated plasma samples were determined using a muVWF- and huVWF antigen ELISA and the results are expressed as a percentage of NMP (*Adamts13*$^{-/-}$) or NHP VWF antigen levels. The muVWF levels of NMP and huVWF levels of NHP were set to 100%. At baseline, control mice demonstrated a mean muVWF antigen level of 91 ± 12 % and the NAC-treated group had 92 ± 18 % muVWF. The muVWF antigen levels of control and NAC-treated mice had increased significantly (P<0.001), 24 hours after rVWF injection (control: 225 ± 64 %; NAC: 179 ± 35 %) but there were no significant differences among groups at this sampling time (Figure 9.13). For the huVWF antigen levels at 24 hours, no significant difference could be found as well (control: 302 ± 253 %; NAC: 254 ± 194 %) (Figure 9.14).

These results demonstrate that the administration of NAC, when TTP symptoms are already present, does not reduce or prevent the increase of murine VWF antigen levels and does not reduce recombinant human VWF antigen levels in a congenital mouse model for TTP.
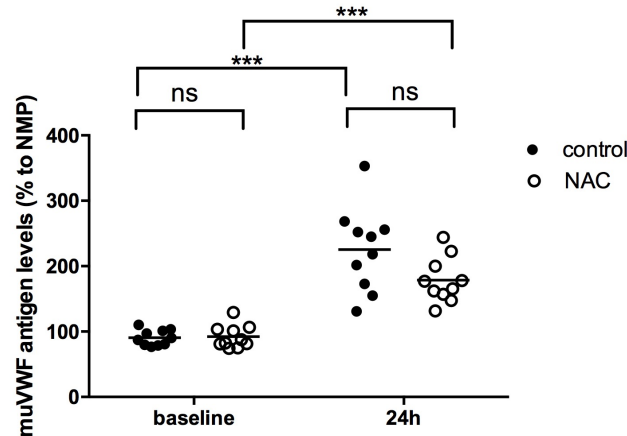
Figure 9.13: Treatment with NAC is not effective in reducing muVWF levels in mice. 800 mg/kg NAC (or saline in controls) was administred one and 12 hours after injection of rVWF. muVWF antigen levels in citrated plasma samples were determined at baseline and 24 hours after rVWF injection using ELISA and compared to the percentage of VWF in NMP. Significance levels are indicated by asterixes (*<0.05, **<0.01, ***<0.001).
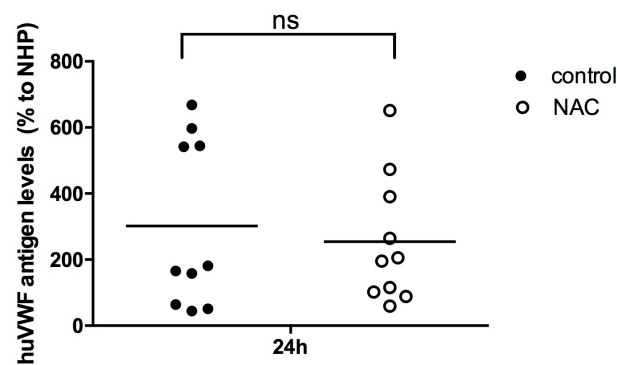
Figure 9.14: Treatment with NAC is not effective in reducing recombinant huVWF levels in mice. 800 mg/kg NAC (or saline in controls) was administred one and 12 hours after injection of rVWF. rVWF antigen levels in citrated plasma samples were determined at baseline and 24 hours after rVWF injection using ELISA and compared to the percentage of VWF in NHP. Significance levels are indicated by asterixes (*<0.05, **<0.01, ***<0.001).

9.2.3 VWF multimer pattern

It was also investigated if NAC administration is effective in reducing VWF multimer size in mice when TTP symptoms are already present. Plasma samples were obtained 6 hours after rVWF injection (control: $n = 5$; NAC: $n = 5$). The average percentage of HMW VWF multimers of NAC-treated mice (31.96 ± 6.21 %) was lower compared to the mean HMW VWF multimer percentage of control mice (24.5 ± 9.74 %). However, not all NAC-treated mice exhibited a reduced percentage of HMW VWF multimers (Figure 9.15, Figure 9.16). Because of the low number of test subjects, these results should be interpreted more as indicative rather than statistically significant.

These results demonstrate that NAC is able to reduce VWF multimer size in some (but not all) mice, 6 hours after rVWF injection. Interestingly, the NAC-treated mice with the highest reduction in HMW VWF multimers did not suffer from TTP, as a normal platelet count (601 x 10^3 platelets/µL) and Hb level (11.4 g/dL) was observed.
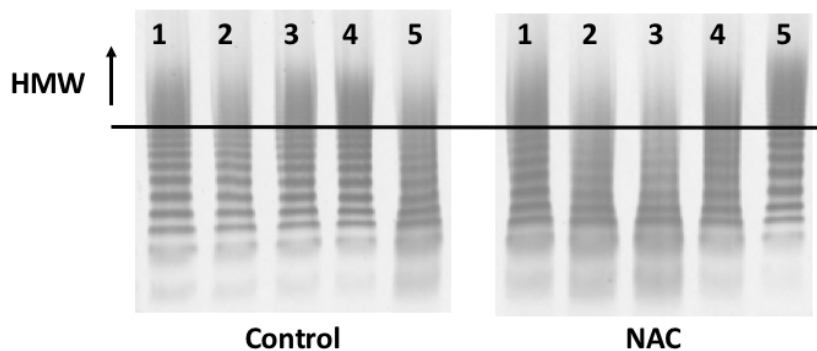
Figure 9.15: VWF multimer size is reduced in some NAC-treated mice, 6 hours after rVWF injection. 800 mg/kg NAC (or saline in controls) was administred one hour after injection of rVWF. 1 µL citrated plasma, obtained 6 hours after rVWF injection was loaded on a 1.2% multimer agarose gel. An image of the multimer agarose gels is displayed for control mice ($n = 5$, left) and mice that received prophylactic NAC ($n = 5$, right).
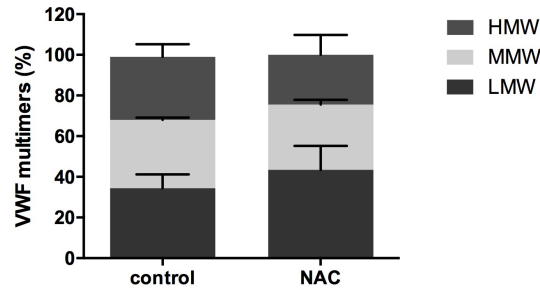
Figure 9.16: The percentage of HMW, MMW and LMW VWF multimers of mice treated with NAC, 6 hours after rVWF injection. VWF multimer analysis was performed and the percentage HMW, MMW and LMW multimers were calculated using densitometry analysis ($n = 5$).

In conclusion, the administration of 800 mg/kg NAC to a congenital TTP mouse model is not effective in resolving TTP symptoms, including thrombocytopenia and tissue damage. Furthermore, it is not effective in reducing VWF antigen levels. In some NAC-treated mice, however, a reduction in VWF multimer size was observed.

It was hypothesized that NAC is not able to cure TTP symptoms in mice because it is only able to reduce VWF multimer size in circulation and not in already existing VWF- and platelet-rich microthrombi. This hypothesis was tested in vitro, by adding NAC to a VWF-containing platelet agglutinate as described in the following section.

9.3 Platelet agglutinate breakdown

The breakdown of a VWF-containing platelet agglutinate by NAC was tested in vitro. A platelet agglutinate was formed using NHP or baboon plasma and ristocetin. Thereafter, 0 mM ($n = 1$) or 32 mM NAC ($n = 3$) was added when agglutination was at a maximum. The addition of 32 mM NAC could not break down the platelet agglutinate (Figure 9.17, Figure 9.18).

These results indicate that NAC is not able to resolve a platelet agglutinate when VWF is already incorporated.
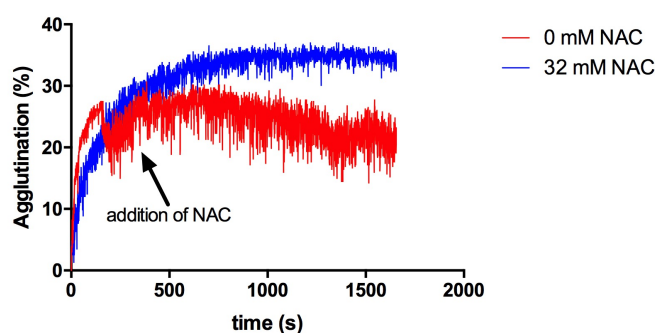
Figure 9.17: NAC is not effective in resolving a platelet agglutinate formed with NHP. First, platelet agglutination was induced and thereafter, 0 mM or 32 mM NAC was added. Representative traces are shown.
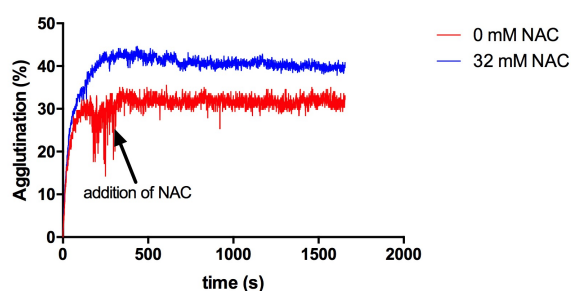
Figure 9.18: NAC is not effective in resolving a platelet agglutinate formed with baboon plasma. First, platelet agglutination was induced and thereafter, 0 mM or 32 mM NAC was added. Representative traces are shown.

Chapter 10

Discussion

Current potential treatments for acute TTP include plasma infusion for congenital TTP patients and plasma exchange, often combined with immunosuppressive therapies like rituximab, (methyl)prednisone and vincristine, for acquired TTP patients. Although plasma therapy reduced the mortality rate of these patients from 90 to less than 20 percent, this treatment also has major disadvantages. Plasma therapy is inconvenient, expensive, requires specialized equipment and nursing, is not always effective and is not without risk. Minor and major complications including haemorrhage, sepsis, cardiac arrest and death are observed (George, 2010). Therefore, new treatment strategies are highly desirable.

10.1 Functionality of NAC

NAC has a free thiol group, which enables it to reduce disulphide bonds. This property of NAC is already being used to treat patients with congestive and obstructive lung diseases. NAC is capable of decreasing mucin- size and viscosity in these patients by reducing disulphide bonds connecting mucin monomers (Sheffner et al., 1964).

Mucin multimers are being formed in a similar manner as VWF. Mucin monomers are translocated to the ER immediately after synthesis, where they form dimers through the C-terminal CK-domains. Next, mucin dimers are transported to the golgi apparatus, where they multimerize through the formation of N-terminal disulphide bonds. Mucin is extensively glycosylated during its multimerization (Perez-Vilar and Hill, 1999). As described in section 2.1, VWF also forms dimers in the ER by 'tail-to-tail' associations and multimerizes in the golgi apparatus by 'head-to-head' associations (Figure 2.1). Because of these similarities, Chen et al. (2011) explored the viability of NAC for reducing VWF size and, consequently, VWF activity. They demonstrated that NAC has multiple effects that could be of benefit for the treatment of TTP, including the reduction of VWF multimer size (in vitro and in mice), the removal of UL-VWF strings from the endothelial surface, the inhibition of VWF-dependent platelet aggre-

gation and collagen binding and the diminished calcium ionophore-induced thrombus formation in mesenteric venules.

Because NAC is a readily available, relatively inexpensive, safe FDA-approved drug and the reducing effect of NAC on the activity and size of human plasma VWF and murine VWF has already been shown (Chen et al., 2011), several acute TTP patients have been treated with this drug. However, the outcome of this therapy for the treatment of acute TTP symptoms was variable (Li et al., 2014; Shortt et al., 2014; Rottenstreich et al., 2015; Cabanillas and Popescu-Martinez, 2015). In these cases, NAC was tested in addition to the existing plasma exchange therapy (and concomitant immunosuppressive therapies). In the case studies of Chapin et al. (2012) and Shortt et al. (2013), two patients suffering from severe TTP symptoms failed to respond to NAC treatment. In the studies of Li et al. (2014) and Rottenstreich et al. (2015) however, four TTP patients were succesfully treated with NAC. These patients first received a bolus injection followed by an infusion of 150 mg/kg or 300 mg/kg NAC per day, a higher dose than in the case study of Shortt et al. (2013). In the case study of Cabanillas and Popescu-Martinez (2015) a relapsing patient went in complete remission after treatment with NAC.

In the current study, the effect of NAC on TTP symptoms, in the absence of other treatment strategies, was investigated in a congenital TTP mouse model. In a parallel project, the effect of NAC on the treatment of TTP in an acquired TTP baboon model was investigated.

10.2 In vitro effect of NAC on plasma VWF

First, the results obtained by Chen et al. (2011), concerning the VWF multimer pattern of NHP after pre-incubation with different concentrations of NAC, were repeated. The observed concentration-dependent reduction in VWF multimer size was comparable to the results described by Chen et al. (2011). Next, the effect of NAC on NMP and baboon plasma VWF multimer size was tested, which also resulted in a concentration-dependent reduction. In addition, the ability of NAC to impair VWF ristocetin/botrocetin cofactor activity using NHP, baboon and NMP plasma was investigated. This interaction is most functional in the presence of HMW VWF multimers (Fischer et al., 1996; Federici et al., 1989). Furthermore, NAC is able to disrupt the intrachain disulphide bond of the VWF A1 domain, inhibiting platelet GPIb binding

(Chen et al., 2011). Therefore, a considerable effect of NAC on VWF activity was assumed. Indeed, experimental results proved that the ristocetin/botrocetin cofactor activity of VWF is also reduced in a concentration-dependent way. Chen et al. (2011) also demonstrated that the pre-incubation of NAC with NHP reduces ristocetin-dependent platelet agglutination in a concentration-dependent manner. These experiments were repeated, using NHP and baboon plasma, and their results were confirmed by comparison to the experimentally observed data. The formation of a VWF-containing platelet agglutinate using botrocetin and NMP still needs optimisation.

These results demonstrate that NAC reduces VWF- multimer size and activity in plasma from humans, baboons and mice. However, a much higher concentration of NAC is required to have a significant effect on murine plasma VWF- multimer size and activity compared to human and baboon plasma VWF. Nevertheless, NAC is able to reduce murine and baboon VWF- multimer size and activity, which is the foundation for the in vivo murine and baboon experiments.

10.3   Effect of NAC on TTP symptoms in mice

The prophylactic administration of NAC before triggering TTP in $Adamts13^{-/-}$ mice was effective in preventing severe symptoms including thrombocytopenia, hemolytic anemia and tissue damage. In addition, mice that received prophylactic NAC indicated a reduction in HMW VWF multimers, when plasma was obtained 6 hours after rVWF injection. This corresponds to the results obtained by Chen et al. (2011), where a reduction of HMW VWF multimers was observed 4 and 8 hours after injection of 800 mg/kg NAC. On the other hand, the administration of NAC after inducing TTP in $Adamts13^{-/-}$ mice could not treat TTP symptoms, including thrombocytopenia and tissue damage. However, a reduction in HMW VWF multimers was also observed in some of these mice. Therefore, it was deduced that NAC is only able to reduce disulphide bonds in circulating VWF multimers but not in already existing VWF- and platelet-rich microthrombi. This hypothesis was confirmed by the inability of NAC to break down VWF-containing platelet agglutinates in vitro, using NHP and baboon plasma. However, this experiment still needs optimisation using NMP and botrocetin.

In addition to a reduction of HMW VWF multimers, significantly lower levels of muVWF- and huVWF antigen levels were demonstrated in mice that received NAC

prophylactically. This could be caused by an increased clearance of VWF due to the loss of HMW VWF multimers, as seen in the case of an increased ADAMTS13 activity (Pruss et al., 2012; Shida et al., 2013). However, previous work in VWF knockout mice showed no influence of multimer size on VWF clearance (Lenting et al., 2004). Furthermore, endogenous VWF levels can increase in the case of TTP due to endothelial cell activation caused by tissue damage (de Wit et al., 2003). As mice that received prophylactic NAC did not demonstrate high levels of tissue damage, this could have prevented the increase of muVWF levels. The reduced VWF antigen levels could therefore have had an effect in the prevention of TTP symptoms, as high levels of HMW VWF are required to develop TTP in this mouse model.

The use of this well-established congenital mouse model for TTP has several advantages and disadvantages as some features resemble human TTP and others are dissimilar. The major clinical features associated with human TTP, including thrombocytopenia, hemolytic anemia and tissue damage, are also present in this mouse model. Furthermore, myocardial lesions that are often observed in this model resemble the lesions of human patients. However, brain- and kidney lesions, which are typically observed in human TTP patients, are not present in this model. The *Adamts13* knockout mice used for this model only develop acute TTP when an external trigger is used. However, congenital TTP patients sometimes develop spontaneous acute TTP. In addition, the use of rVWF as an external trigger for TTP is not physiologically relevant. Triggers in patients are for example pregnancy, infection, trauma and surgical procedures, leading to endothelial activation and subsequent UL-VWF release. Another difference between human TTP and this mouse model is that mice do not reach the end-stage of the disease, as they return to normal within 14 days (Schiviz et al., 2012; Vanhoorelbeke and De Meyer, 2013). Another limitation of this mouse model is that NAC is only administered using bolus injections instead of continuous infusions. However, patients with acetaminophen overdose are preferably treated with continuous infusions of NAC. Therefore, it would be worthwhile to investigate if the administration of NAC using an implantable continuous infusion osmotic pump in this congenital TTP mouse model is favourable for the treatment of TTP.

10.4   Effect of NAC on TTP symptoms in baboons

Before the start of this thesis research, the treatment of acute TTP symptoms using NAC in a baboon model for acquired TTP was investigated by the Laboratory for Thrombosis Research at the KU Leuven Kulak. This model is more easily translatable to the clinical situation given the closer resemblance of non-human primates to humans. In this model, the injection of the inhibitory anti-ADAMTS13 antibody 3H9, directed against the metalloprotease domain, results in the spontaneous development of TTP symptoms including severe thrombocytopenia, hemolytic anemia (represented by decreased Hb levels and an increased amount of schistocytes) and tissue damage (represented by increased LDH activity levels) (Feys et al., 2010b). In this study, 3H9 was intravenously injected every 48 hours at a concentration of 600 µg/kg which caused ADAMTS13 activity to fell below detection limit. After 4 days, the baboons suffered from deep thrombocytopenia, hemolytic anemia and tissue damage. To investigate the effect of NAC on the treatment of these symptoms, 4 baboons were intravenously injected with NAC every 12 hours at a concentration of 400 mg/kg, from day 4 up to day 9. As a control, 4 baboons were injected with equal volumes of saline. Platelet counts, Hb levels, schistocyte amounts and LDH activity levels from treated and untreated baboons remained comparable during the study. Thrombocytopenia, hemolytic anemia and tissue damage were severely present in this baboon model for TTP and NAC was not able resolve these symptoms. On the other hand, VWF antigen levels and HMW VWF multimers were decreased in NAC-treated baboons, indicating that NAC was able to reduce disulphide bonds in circulating VWF.

These results are comparable to the results obtained in the congenital TTP mouse model, after treatment with NAC. On the other hand, significantly reduced VWF antigen levels in NAC-treated mice compared to control mice were not observed, 24 hours after rVWF injection. In addition, significantly increased Hb levels compared to control mice were observed in NAC-treated mice, 24 hours after rVWF injection.

In contrast to the congenital TTP mouse model, the prophylactic administration of NAC was not tested in the baboon model for acquired TTP and it would be interesting to perform this.

10.5 Other characteristics of NAC

In addition to reducing disulphide bonds of VWF, NAC exhibits other effects that impair platelet aggregation. For example, NAC is able to inhibit platelet aggregation induced by adenosine diphosphate or collagen in a concentration-dependent way in vitro (Chen et al., 2011). It is also able to increase the inhibition of platelet aggregation induced by the smooth muscle relaxant nitroglycerin (Loscalzo, 1985) or by improving the bioavailability of platelet nitric oxide, a platelet inhibitor (Anfossi et al., 2001).

Furthermore, NAC has antioxidative and free radical scavenger properties. These effects are achieved by the hydrolysis of NAC to cysteine and the subsequent conversion to GSH. GSH is important for the protection of the human body against oxidative damage, caused by reactive oxygen species (ROS). However, the production of GSH is often limited by the availability of cysteine (Arakawa and Ito, 2007) but NAC is able to correct or prevent this GSH depletion. For example, NAC is able to block the ROS-induced apoptosis in human umbilical vein endothelial cells (Galle et al., 1999) or to protect human primary gingival fibroblast against ROS-induced cytotoxicity (Spagnuolo et al., 2006). It is also able to impair ROS-mediated ER stress during liver ischemia-reperfusion injury in mice (Sun et al., 2014) and during cerebral ischemia and reperfusion injury in rats (Sekhon et al., 2003). Until now, no connection between TTP and ROS generation has been found. However, it has been shown that ROS generation is present during ischemia (Becker, 2004). Since microthrombi can cause ischemia, NAC could be potentially beneficent as a ROS scavenger in TTP.

A possible adverse effect of NAC is an increased bleeding risk, as significant decreases in plasma levels of vitamin K-dependent hemostatic proteins and a corresponding prolonged prothrombin time are observed in humans, after the intravenously infusion of NAC (Jepsen and Hansen, 1994; Knudsen et al., 2005; Niemi et al., 2006). However, NAC has no effect on tail-vein bleeding times in $Adamts13^{-/-}$ mice (Chen et al., 2011) and on bleeding times in baboons with acquired TTP (Tersteeg et al., unpublished results). In addition, a potential adverse effect of NAC observed in mice after chronic, high-dose administration is pulmonary hypertension (Palmer et al., 2007). Therefore, caution is necessary when increasing the NAC dosage.

10.6 Clinical trial: NAC administration to TTP patients

Currently, the clinical pilot study: N-acetylcysteine in suspected thrombotic thrombocytopenic purpura, is recruiting patients (Clinicaltrials.gov ID: NCT01808521). The trial will investigate if the intravenous administration of NAC can decrease complications in TTP patients receiving plasma exchange therapy. This will be achieved by measuring platelet counts, VWF- and ADAMTS13 activity and red blood cell hemolysis. NAC (Acetadote) will be administred daily, starting after the first plasma exchange. The dose used for acetaminophen overdose will be adopted: a 150 mg/kg loading bolus followed by 150 mg/kg over 17 hours. Although the results of this thesis demonstrated that NAC is not able to treat acute TTP symptoms in mice and baboons, it could be of potential benefit for acute TTP patients, when used in combination with plasma exchange therapy.

10.7 General conclusion

In conclusion, NAC is not effective in treating acute TTP in preclinical animal models (congenital TTP mouse model and acquired TTP baboon model). Therefore, there is no evidence that suggests NAC would be beneficial for the treatment of acute TTP patients. However, the prophylactic administration of NAC was able to prevent the onset of severe TTP symptoms in the congenital TTP mouse model. Consequently, the prophylactic administration of NAC to relapsing patients could be effective in preventing the onset of new TTP episodes.

References

[1] Akiyama, M., Takeda, S., Kokame, K., Takagi, J. & Miyata, T. (2009). Crystal structures of the noncatalytic domains of ADAMTS13 reveal multiple discontinuous exosites for von Willebrand factor. Proceedings of the National Academy of Sciences of the United States of America, 106(46): 19274-19279.

[2] Anfossi, G., Russo, I., Massucco, P., Mattiello, L., Cavalot, F., Trovati, M. (2001). N-acetyl-L-cysteine exerts direct anti-aggregating effect on human platelets. Eur J Clin Invest, 31(5):452461.

[3] Arakawa, M. & Ito, Y. (2007). N-acetylcysteine and neurodegenerative diseases: basic and clinical pharmacology. Cerebellum, 6(4): 308-314.

[4] Becker, L.B. (2004). New concepts in reactive oxygen species and cardiovascular reperfusion physiology. Cardiovascular Research, 61: 461-470.

[5] Blombery, P. & Scully, M. (2014). Management of thrombotic thrombocytopenic purpura: current perspectives. Journal of Blood Medicine, 5: 15-23

[6] Bork, P., & Beckmann, G. (1993). The CUB domain – a widespread module in developmentally–regulated proteins. Journal of Molecular Biology, 231(2): 539-545.

[7] Cabanillas, G., Popescu-Martinez, A. (2015). N-acetylcysteine for Relapsing Thrombotic Thrombocytopenic Purpura: More Evidence of a Promising Drug. Am J Ther, Epub 2015.

[8] Callewaert, F., Roodt, J., Ulrichts, H., et al. (2012). Evaluation of efficacy and safety of the anti-VWF Nanobody ALX-0681 in a preclinical baboon model of acquired thrombotic thrombocytopenic purpura. Blood, 120(17): 3603-3610.

[9] Cataland, S.R., Peyvandi, F., Mannucci, P.M., et al. (2012). Initial experience from a double-blind, placebo-controlled, clinical outcome study of ARC1779 in patients with thrombotic thrombocytopenic purpura. American Journal of Hematology, 87(4): 430-432.

[10] Chapin, J., Weksler, B., Magro, C., Laurence, J. (2012). Eculizumab in the treatment of refractory idiopathic thrombotic thrombocytopenic purpura. Br J Haematol, 157: 772-774.

[11] Chapin, J.C. & Hajjar, K.A. (2015). Fibrinolysis and the control of blood coagulation. Blood Reviews, 29(1): 17-24.

[12] Chen, J., Reheman, A., Gushiken, F.C., et al. (2011). N-acetylcysteine reduces the size and activity of von Willebrand factor in human plasma and mice. Journal of Clinical Investigation, 121(2): 593-603.

[13] Coppo, P. & Veyradier, A. (2012). Current management and therapeutical perspectives in thrombotic thrombocytopenic purpura. La Presse Mdicale, 41(3): e163-e176.

[14] Crawley, J.T.B., Lam, J.K., Rance, J.B., Mollica, L.R., O'Donnell, J.S. & Lane, D.A. (2005). Proteolytic inactivation of ADAMTS13 by thrombin and plasmin. Blood, 105(3): 1085-1093.

[15] Crawley, J.T.B., de Groot, R., Xiang, Y., Luken, B.M. & Lane, D.A. (2011). Unraveling the scissile bond: how ADAMTS13 recognizes and cleaves von Willebrand factor. Blood, 118(12): 3212-3221.

[16] De Ceunynck, K., De Meyer, S.F., Vanhoorelbeke, K. (2013). Unwinding the von Willebrand factor strings puzzle. Blood, 121(2): 270-277.

[17] Deforche, L., Roose, E., Vandenbulcke, A., et al. (2015). Linker regions and flexibility around the metalloprotease domain account for conformational activation of ADAMTS-13. Journal of Thrombosis and Haemostasis, 13(11): 2063-2075

[18] de Groot, R., Bardhan, A., Ramroop, N., Lane, D.A. & Crawley, J.T.B. (2009). Essential role of the disintegrin-like domain in ADAMTS13 function. Blood, 113(22): 5609-5616.

[19] de Groot, R., Lane, D.A. & Crawley, J.T.B. (2010). The ADAMTS13 metalloprotease domain: roles of subsites in enzyme activity and specificity. Blood, 116(16): 3064-3072.

[20] de Groot, R., Lane, D.A., & Crawley, J.T.B. (2015). The role of the ADAMTS13 cysteine-rich domain in VWF binding and proteolysis. Blood, 125(12): 1968-1975.

[21] De Meyer, S.F., Deckmyn, H. & Vanhoorelbeke, K. (2009). Von Willebrand factor to the rescue. Blood, 113(21): 5049-5057.

[22] de Wit, T.R., Fijnheer, R., Brinkman, H.J., Kersting, S., Hene, R.J., Mourik, J.A. (2003). Endothelial cell activation in thrombotic thrombocytopenic purpura (TTP): a prospective analysis. Britisch Journal of Haematology, 123: 522-527.

[23] Di Stasio, E., Romitelli, F., Lancellotti, S., Arcovito, A., Giardina, B., De Cristofaro, R. (2009). Kinetic study of von Willebrand factor self-aggregation induced by ristocetin. Biophysical Chemistry, 144(3): 101-107.

[24] Dong, J.F., Moake, J.L., Nolasco, L., et al. (2002). ADAMTS-13 rapidly cleaves newly secreted ultralarge von Willebrand factor multimers on the endothelial surface under flowing conditions. Blood, 100(12): 4033-4039.

[25] Federici, A.B., Bader, R., Pagani, S., Colibretti, M.L., De Marco, L., Mannucci, P.M. (1989). Binding of von Willebrand factor to glycoproteins Ib and IIb/IIIa complex: affinity is related to multimeric size. Br J Haematol, 73: 93-9.

[26] Ferrari, S., Scheiflinger, F., Rieger, M., et al. (2007). Prognostic value of anti-ADAMTS13 antibody features (Ig isotype, titer, and inhibitory effect) in a cohort of 35 adult French patients undergoing a first episode of thrombotic microangiopathy with undetectable ADAMTS13 activity. Blood, 109(7): 2815-2822.

[27] Ferrari, S., Mudde, G.C., Rieger, M., Veyradier, A., Hovinga, J.A.K. & Scheiflinger, F. (2009). IgG subclass distribution of anti-ADAMTS13 antibodies in patients with acquired thrombotic thrombocytopenic purpura. Journal of Thrombosis and Haemostasis, 7(10): 1703-1710.

[28] Feys, H.B, Liu,F., Dong, N., Pareyn, I., Vauterin, S., Vandeputte, N., Noppe, W., Ruan, W., Deckmyn, H., Vanhoorelbeke, K. (2006). ADAMTS-13 plasma level determination uncovers antigen absence in acquired thrombotic thrombocytopenic purpuraand ethnic differences. Journal of Thrombosis and Haemostasis, 4: 955-962.

[29] Feys, H.B., Anderson, P.J., Vanhoorelbeke, K., Majerus, E.M. & Sadler, J.E. (2009). Multi-step binding of ADAMTS-13 to von Willebrand factor. Journal of Thrombosis and Haemostasis, 7(12): 2088-2095.

[30] Feys, H.B., Vandeputte, N., Palla, R., et al. (2010). Inactivation of ADAMTS13 by plasmin as a potential cause of thrombotic thrombocytopenic purpura. Journal of Thrombosis and Haemostasis, 8(9):2053-2062.

[31] Feys, H.B., Roodt, J., Vandeputte, N., et al. (2010). Thrombotic thrombocytopenic purpura directly linked with ADAMTS13 inhibition in the baboon (Papio ursinus). Blood, 116(12): 2005-2010.

[32] Feys, H.B., Roodt, J., Vandeputte, N., et al. (2012). Inhibition of von Willebrand factor-platelet glycoprotein Ib interaction prevents and reverses symptoms of acute acquired thrombotic thrombocytopenic purpura in baboons. Blood, 120(17): 3611-3614.

[33] Fischer, B.E., Kramer, G., Mitterer, A., Grillberger, L., Reiter, M., Mundt, W., Dorner, F., Eibl, J. (1996). Effect of multimerization of human and recombinant von Willebrand factor on platelet aggregation, binding to collagen and binding of coagulation factor VIII. Thromb Res, 84: 55-66.

[34] Gale, A.J. (2011). Current understanding of hemostasis. Toxicol Pathol, 39(1): 273-280.

[35] Galle, J., Heermeier, K., Wanner, C. Atherogenic lipoproteins, oxidative stress, and cell death. Kidney Int. Suppl, 71:S62-5.

[36] Gardner, M.D., Chion, C.K.N.K., de Groot, R., Shah, A., Crawley, J.T.B. & Lane, D.A. (2009). A functional calcium-binding site in the metalloprotease domain of ADAMTS13. Blood, 113(5): 1149-1157.

[37] George, J.N. (2010). How I treat patients with thrombotic thrombocytopenic purpura:2010. Blood, 116(20): 4060-4069

[38] Heard, K.J. (2008). Acetylcysteine for acetaminophen poisoning. New England Journal of Medicine, 359(3): 285-292.

[39] Hernandez-Zamora, E., Zavala-Hernandez, C., Quintana-Gonzalez, S. & Reyes-Maldonado, E. (2015). Von Willebrand disease. Molecular biology and diagnosis, 83(3): 255-264.

[40] Hovinga, J.A.K. & Lammle, B. (2012). Role of ADAMTS13 in the pathogenesis, diagnosis, and treatment of thrombotic thrombocytopenic purpura. Hematology-American Society of Hematology Education Program, 2012: 610-616.

[41] Jepsen, S. & Hansen, A.B. (1994). The influence of N-acetylcysteine on the measurement of prothrombin time and activated partial thromboplastin time in healthy subjects. Scand J Clin Lab Invest, 54(7): 543-7.

[42] Knudsen, T.T., Thorsen, S., Jensen, S.A., Dalhoff, K., Schmidt, L..E., Becker, U., Bendtsen, F. (2005). Effect of intravenous N-acetylcysteine infusion on haemostatic parameters in healthy subjects. Gut, 54: 515-521.

[43] Lammle, B., Hovinga, J.A.K. & Alberio, L. (2005). Thrombotic thrombocytopenic purpura. Journal of Thrombosis and Haemostasis, 3(8): 1663-1675.

[44] Lenting, P.J., Westein, E., Terraube, V., Ribba, A.S., Huizinga, E.G., Meyer, D., de Groot, P.G., Denis, C.V. (2004). An experimental model to study the in vivo survival of von willebrand factor. basic aspects and application to the R1205H mutation. J Biol Chem, 279: 12102-12109.

[45] Lenting, P.J., Casari, C., Christophe, O.D. & Denis, C.V. (2012). Von Willebrand factor: the old, the new and the unknown. Journal of Thrombosis and Haemostasis, 10(12): 2428-2437.

[46] Levy, G.G., Nichols, W.C., Lian, E.C., et al. (2001). Mutations in a member of the ADAMTS gene family cause thrombotic thrombocytopenic purpura. Nature, 413(6855):488-494.

[47] Li, G.W., Rambally, S., Kamboj, J., et al. (2014). Treatment of refractory thrombotic thrombocytopenic purpura with N-acetylcysteine: a case report. Transfusion, 54(5): 1221-1224.

[48] Loscalzo, J. (1985). N-Acetylcysteine potentiates inhibition of platelet aggregation by nitroglycerin. J Clin Invest, 76(2):703708.

[49] Luken, B.M., Turenhout, E.A.M., Hulstein, J.J.J., Van Mourik, J.A., Fijnheer, R. & Voorberg, J. (2005). The spacer domain of ADAMTS13 contains a major binding site for antibodies in patients with thrombotic thrombocytopenic purpura. Journal of Thrombosis and Haemostasis, 93(2): 267-274.

[50] Luo, G.P., Ni, B., Yang, X., Wu & Y.Z. (2012). Von Willebrand Factor: More Than a Regulator of Hemostasis and Thrombosis. Acta Haematologica, 128(3): 158-169.

[51] Meitinger, T., Meindl, A., Bork, P., et al. (1993). Molecular modeling of the norrie disease protein predicts a cystine knot growth-factor tertiary structure. Nature Genetics, 5(4): 376-380.

[52] Moake, J.L. (2002). Mechanisms of disease - Thrombotic microangiopathies. New England Journal of Medicine, 347(8): 589-600.

[53] Motto, D., Chauhan, A., Zhu, G., et al. (2005). Shigatoxin triggers thrombotic thrombocytopenic purpura in genetically susceptible ADAMTS13-deficient mice. J Clin Invest, 115(10): 2752-2761.

[54] Muia, J., Zhu, J., Gupta, G., et al. (2014). Allosteric activation of ADAMTS13 by von Willebrand factor. Proceedings of the National Academy of Sciences of the United States of America, 111(52): 18584-18589.

[55] Niemi, T.T., Munsterhielm, E., Poyhia, R., Hynninen, M.S., Salmenpera, M.T. (2006). The effect of N-acetylcysteine on blood coagulation and platelet function in patients undergoing open repair of abdominal aortic aneurysm. Blood Coagul Fibrinolysis, 17(1): 29-34.

[56] Nishio,K., Anderson, P.J., Zheng, X.L. & Sadler, J.E. (2004). Binding of platelet glycoprotein Ib alpha to von Willebrand factor domain A1 stimulates the cleavage of the adjacent domain A2 by ADAMTS13. Proceedings of the National Academy of Sciences of the United States of America, 101(29): 10578-10583.

[57] Palmer, L.A., Doctor, A., Chhabra, P., Sheram, M.L., Laubach, V.E., Karlinsey, M.Z., Forbes, M.S., Macdonald, T., Gaston, B. (2007). S-nitrosothiols signal hypoxia-mimetic vascular pathology. J Clin Invest, 117(9): 2592-601.

[58] Perez-Vilar, J. & Hill, R.L. (1999). The structure and assembly of secreted mucins. J Biol Chem, 274(45): 31751-31544

[59] Peyvandi, F., Scully, M., Hovinga, J.A.K., et al. (2016). Caplacizumab for Acquired Thrombotic Thrombocytopenic Purpura. New England Journal of Medicine, 374(6): 511-522.

[60] Pimanda, J.E., Ganderton, T., Maekawa, A., et al. (2004). Role of thrombospondin-1 in control of von Willebrand factor multimer size in mice. Journal of Biological Chemistry, 279(20): 21439-21448.

[61] Plaimauer, B., Hovinga, J.A.K., Juno, C., et al. (2011). Recombinant ADAMTS13 normalizes von Willebrand factor-cleaving activity in plasma of acquired TTP patients by overriding inhibitory antibodies. Journal of Thrombosis and Haemostasis, 9(5): 936-944.

[62] Pruss, C.M., Golder, M., Bryant, A., Hegadorn, C. Haberichter, S., Lillicrap, D. (2012). Use of a mouse model to elucidate the phenotypic effects of thevon Willebrand factor cleavage mutants, Y1605A/M1606A and R1597W. Journal of Thrombosis and Haemostasis, 10(5): 940-950

[63] Rottenstreich, A., Hochberg- Klein, S., Rund, D. & Kalish, Y. (2015). The role of N-acetylcysteine in the treatment of thrombotic thrombocytopenic purpura. J Thromb Thrombolysis, 2015: 1-6.

[64] Ruggeri, Z.M. (2007). The role of von Willebrand factor in thrombus formation. Thrombosis Research, 120: S5-S9.

[65] Sadler, J.E. (1998). Biochemistry and genetics of von Willebrand factor. Annual Review of Biochemistry, 67: 395-424.

[66] Sadler, J.E. (2005). Von Willebrand factor: two sides of a coin. Journal of Thrombosis and Haemostasis, 3(8): 1702-1709.

[67] Sadler, J.E. (2008). Von Willebrand factor, ADAMTS13, and thrombotic thrombocytopenic purpura. Blood, 112(1): 11-18.

[68] Scheiflinger, F., Knobl, P., Trattner, B., et al. (2013). Nonneutralizing IgM and IgG antibodies to von Willebrand factor-cleaving protease (ADAMTS-13) in a patient with thrombotic thrombocytopenic purpura. Blood, 102(9): 3241-3243

[69] Schiviz, A., Wuersch, K., Piskernik, C., et al. (2012). A new mouse model mimicking thrombotic thrombocytopenic purpura: correction of symptoms by recombinant human ADAMTS13. Blood, 119(25): 6128-6135.

[70] Schulze, H. & Shivdasani, R.A. (2005). Mechanisms of thrombopoiesis. Journal of Thrombosis and Haemostasis, 3(8): 1717-1724.

[71] Scully, M., McDonald, V., Cavenagh, J., et al. (2011). A phase 2 study of the safety and efficacy of rituximab with plasma exchange in acute acquired thrombotic thrombocytopenic purpura. Blood, 118(7):1746-1753.

[72] Sekhon, B., Sekhon, C., Khan, M., Patel, S.J., Singh, I., Singh, A.K. (2003). N-Acetyl cysteine protects against injury in a rat model of focal cerebral ischemia. Brain Res, 971(1): 1-8.

[73] Sheffner, A.L., Medler, E.M., Jacobs, L.W., Sarett, H.P. (1964). The in vitro reduction in viscosity of human tracheobronchial secretions by acetylcysteine. Am Rev Respir Dis, 90: 721-729.

[74] Shida, Y., Brown, C., Mewburn, J., Sponagle, K., Lillicrap, D. (2013). Impact of ADAMTS13-mediated regulation of von Willebrand factor multimer profile on hemostasis and VWF clearance. Journal of Thrombosis and Haemostasis. 11 Suppl 2: 288[abstract OC 91].

[75] Shortt, J., Opat, S.S. & Wood, E.M. (2014). N-Acetylcysteine for thrombotic thrombocytopenic purpura: is a von Willebrand factor-inhibitory dose feasible in vivo? Transfusion, 54(9):2362-2363.

[76] Somerville, R.P.T., Longpre, J.M., Jungers, K.A., et al. (2003). Characterization of ADAMTS-9 and ADAMTS-20 as a distinct ADAMTS subfamily related to Caenorhabditis elegans GON-1. Journal of Biological Chemistry, 278(11): 9503-9513.

[77] South, K., Luken, B.M., Crawley, J.T.B., et al. (2014). Conformational activation of ADAMTS13. Proceedings of the National Academy of Sciences of the United States of America, 111(52): 18578-18583.

[78] Spagnuolo, G., D'Anto, V., Cosentino, C., Schmalz, G., Schweikl, H., Rengo, S. (2006). Biomaterials, 27(9): 1803-9.

[79] Sun, Y., Pu, Y., Lu, L., Wang, X.H., Zhang, F., Rao, J.H. (2014). N-acetylcysteine attenuates reactive-oxygen-species-mediated endoplasmic reticulum stress during liver ischemia-reperfusion injury. World J Gastroenterol, 20(41): 15289-98.

[80] Tersteeg, C., Schiviz, A., De Meyer, S.F., et al. (2015). Potential for Recombinant ADAMTS13 as an Effective Therapy for Acquired Thrombotic Thrombocytopenic Purpura. Arteriosclerosis Thrombosis and Vascular Biology, 35(11): 2336-2342.

[81] Thomas, M.R., de Groot, R., Scully, M.A. & Crawley, J.T.B. (2015). Pathogenicity of Anti-ADAMTS13 Autoantibodies in Acquired Thrombotic Thrombocytopenic Purpura. Ebiomedicine, 2(8): 942-952.

[82] Tsai, H.M. (2010). Pathophysiology of thrombotic thrombocytopenic purpura. International Journal of Hematology, 91(1): 1-19.

[83] Ulrichts, H., Udvardy, M.S., Lenting, P.J., et al. (2006). Shielding of the A1 domain by the D'D3 domains of von Willebrand factor modulates its interaction with platelet glycoprotein Ib-IX-V. Journal of Biological Chemistry, 281(8): 4699-4707.

[84] Ulrichts, H., Silence, K., Schoolmeester, A., et al. (2011). Antithrombotic drug candidate ALX-0081 shows superior preclinical efficacy and safety compared with currently marketed antiplatelet drugs. Blood, 118(3): 757-765.

[85] Vanhoorelbeke, K., Cauwenberghs, N., Vauterin, S., Schlammadinger, A., Mazurier C. & Deckmyn, H. (2000). A reliable and reproducible ELISA method to measure ristocetin cofactor activity of von Willebrand factor. Thrombosis and Haemostasis, 83 (1): 107-113.

[86] Vanhoorelbeke, K. & De Meyer, S.F. (2013). Animal models for thrombotic thrombocytopenic purpura. Journal of Thrombosis and Haemostasis, 11: 2-10.

[87] Wang, A., Liu, F., Dong, N., et al. (2010). Thrombospondin-1 and ADAMTS13 competitively bind to VWF A2 and A3 domains in vitro. Thromb Res, 126(4): e260-e265.

[88] Zhang, Q, Zhou, Y.F., Zhang, C.Z., Zhang, X., Lu, C. & Springer, T.A. (2009). Structural specializations of A2, a force-sensing domain in the ultralarge vascular protein von Willebrand factor. Proceedings of the National Academy of Sciences of the United States of America, 106(23): 9226-9231.

[89] Zheng, X.L., Chung, D., Takayama, T.K., Majerus, E.M., Sadler, J.E. & Fujikawa, K.(2001). Structure of von Willebrand factor-cleaving protease (ADAMTS13), a metalloprotease involved in thrombotic thrombocytopenic purpura. Journal of Biological Chemistry, 276(44): 41059-41063.

[90] Zheng, X.L., Wu, H.M., Shang, D., et al. (2010). Multiple domains of ADAMTS13 are targeted by autoantibodies against ADAMTS13 in patients with acquired idiopathic thrombotic thrombocytopenic purpura. Haematologica-the Hematology Journal, 95(9): 1555-1562.

[91] Zhou, Y.F., Eng, E.T., Zhu, J., Lu, C., Walz, T. & Springer, T.A. (2012). Sequence and structure relationships within von Willebrand factor. Blood, 120(2): 449-458.

Appendix A

Risk Analysis

The Laboratory for Thrombosis Research (Latron) at the KU Leuven Kulak is a laboratory with containment level L1. A lab coat was always worn during the execution of experiments and the products were used in a careful way in order to avoid aerosols and spatters. Gloves were worn when irritating or potentially carcinogenic products were used. This was the case for SDS (E1), OPD (E4), H_2O_2 (E4), H_2SO_4 (E4) and Kerosene (E3). It was also ensured that these products (and other products) were eliminated in the proper waste containers. During the heating of the multimer agarose gel, toxic vapours are released. Therefore, this was always done in a laminar flow cabinet.

During this Master's thesis, animal (mice) experiments were performed. The mice are housed in an A1 animalium. When performing these experiments, a special lab coat and gloves were always worn. This provided protection against bite- and scratch wounds. The exposure to bedding material and urine must be minimized, to avoid the development of allergies. The methods of blood withdrawals and injections were approved by the Institutional Animal Care and Use Committee of KU Leuven (Belgium). The needles and capillaries (glass) were removed in the appropriate waste container and recapping of needles was forbidden. When the animal experiment was completed, an overdose of isoflurane (E3) was administered to the mice. Afterwards, the mouse carcasses were stored in the freezer until the specialised company Rendac removed them.